Attosecond Physics — Theory

Lecture notes 2013
(Work in progress)

Armin Scrinzi

November 19, 2013

DISCLAIMER

Theses are not lecture notes, but rather scribbles.
They need severe revision
There are inconsistencies, errors, some false claims
all things that were put there to be corrected
at one point
in their present status, the notes should not be used for actual computations without verification
I reserve the right not to answer questions related to these notes

Contents

Notation

$\mathcal{E}$	electric field
E_0	ground state energy
ω_l	laser fundamental (circular) frequency
T_l	laser period = laser optical cycle

Chapter 1

Introduction

In the early years of 2000, extremely short, controlled light pulses could be produced for the first time. Typical duration of these pulses is 0.1 fs $= 10^{-16}\,s = 100 \times 10^{-18}\,s = 100$ as with 1 as (attosecond) $= 10^{-18}\,s$.

Except for being short, the timing of these pulses can be controlled on a scale of about 10 as, 1/10 of their typical duration. These are the time scale on which electronic changes in ordinary matter happen. One or two decades earlier, the shortest pulses were in the $\gtrsim 10fs$ regime, the time scale on wich nuclei move during chemical reactions. This had given us the possibilty to directly observe what happens during chemical reactions.

- Atoms
- Molecules
- Solids

Chapter 2

Time scales, key experiments, units

2.1 What happens in an attosecond?

2.1.1 Electronic motion in an atom

Velocity of an electron in the atom

The quantum mechanical **virial theorem** for the Coulomb potential establishes a relation between the kinetic and the potential energy of an electron in an atom. It is strictly valid for any bound state of any Coulombic system:

$$\langle T_{kin} \rangle = -\frac{1}{2} \langle V_{pot} \rangle = E_{bind}. \tag{2.1}$$

For any hydrogen-like ion one can relate the binding energy to the kinetic energy of a *single* electron. As E_{bind} is easily determined experimentally.

The average velocity v_0 of the electron in the ground state of the atom is

$$T_{kin} = \frac{m_e v_0^2}{2} = E_{bind} = 13.6\, eV \text{ (hydrogen)}. \tag{2.2}$$

The *Rydberg energy* is defined as the binding energy of the hydrogen atom:

$$1\text{Ry} := 13.6058\, eV. \tag{2.3}$$

Thus we find for the velocity

$$v_0 = \sqrt{\frac{2\text{Ry}}{m_e}} = \sqrt{\frac{27.2116\, eV}{0.511\, MeV/c^2}} = \alpha c, \tag{2.4}$$

$\alpha \approx 1/137\ldots$ **fine structure constant,**
$c\ldots$ **velocity of light.**

The typical speed of an electron in an atom is given by

$$v_0 = c/137 = \alpha c. \tag{2.5}$$

It is easy to see that α is indeed exactly the fine-structure constant: expressing everything in terms of proton charge e, electron mass m_e and $\hbar$, e.g. table 2.1.

For non-hydrogen like systems, we cannot associate $\langle T_{kin} \rangle$ with a single electron. Nevertheless, the order of magnitude estimate for the kinetic energy of any valence electron by its ionization potential is valid.

The motion of the electrons in an atom is sub-relativistic on the scale αZ^*, where Z^* is some effective screened charge. For the valence electrons of a neutral $Z^* \sim 1$. For larger atoms only outer electrons can be treated non-relativistically.

Distance of the electron to the nucleus

In order to estimate the radius of the electron orbit, we again use the virial theorem for the Coulomb potential:

$$\langle V_{pot} \rangle = -2\,\mathrm{Ry} = -\frac{e^2}{4\pi\epsilon_0 a_0}, \tag{2.6}$$

where a_0 is the searched for radius. ϵ_0 is the dielectric constant in the vacuum, $\epsilon_0 = 8.85 \cdot 10^{-12} As/Vm$. Hence we get

$$a_0 = \frac{e^2}{8\pi\epsilon_0\,\mathrm{Ry}} \approx 0.529 \times 10^{-10} m \approx 0.05\ nm. \tag{2.7}$$

a_0 is called *Bohr's atomic radius.*

The classical orbit time of a valence electron

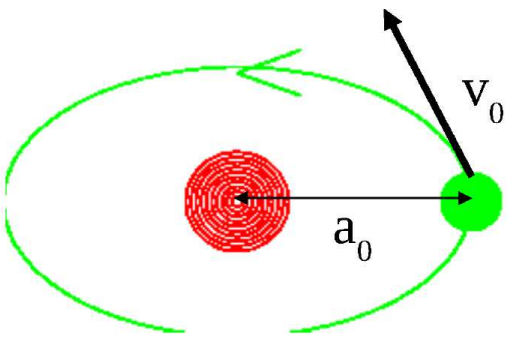

Figure 2.1: An electron as it travels around a nucleus...

If the atom moves with velocity v_0 on a circular orbit with radius a_0 around the nucleus, the orbit time is

$$\tau_{orbit} = \frac{2\pi a_0}{v_0} = 2\pi \frac{0.529 \times 10^{-10}}{3 \times 10^8} \times 137s \approx 2\pi \cdot 24.188 \times 10^{-18} s \approx 150\,as. \tag{2.8}$$

as stands for attosecond $= 10^{-18s}$.

2.1.2 Transition energies — time scales

Electron density of a superposition state

Starting from the Schrödinger equation (with $\hbar = 1$, atomic units)

$$\Big(-\frac{\hbar^2\Delta}{2m} + V(r)\Big)\Psi(r,t) = i\frac{\partial}{\partial t}\Psi(r,t), \tag{2.9}$$

we can make an ansatz for *quasi-stationary* solutions

$$\Psi(r,t) := e^{-iEt}\phi(r), \tag{2.10}$$

with $\phi(r)$ fulfilling the *time independent Schrödinger equation*

$$\Big(-\frac{\hbar^2\Delta}{2m} + V(r)\Big)\phi(t) = E\phi(t). \tag{2.11}$$

Quasi-stationary means that the electron density is time independent,

$$\rho(r) = |\Psi(r,t)|^2 = |\phi(r)|^2. \tag{2.12}$$

If we have a superposition of two such solutions of different energy,

$$\Psi(r,t) = e^{-iE_1t}\phi_1(r) + e^{-iE_2t}\phi_2(r), \tag{2.13}$$

we find for the electron density

$$\rho(r,t) = |\Psi(r,t)|^2 = |\phi_1|^2 + |\phi_2|^2 + \phi_1^*\phi_2 e^{-i(E_2-E_1)t} + h.c. \tag{2.14}$$

Notation: *h.c.* ... "hermitian conjugate" (which is here just the complex conjugate). Notice that the electron density of the superposition of two quasi-stationary states is time dependent. The time dependent part is periodic with a period

$$\tau = \frac{2\pi}{|E_2 - E_1|}. \tag{2.15}$$

Characteristic times of quantum systems

$$\tau \sim \frac{2\pi}{\Delta E} \qquad (\hbar = 1) \tag{2.16}$$

ΔE... characteristic energy differences

	ΔE	τ
vibrational motion of nuclei in molecules	$\sim$ 100 meV	$\sim$ 20 fs
valence electrons in atoms/molecules	13 eV	150 as
inner shell electrons	$\sim$ 1 keV	$\sim$ 2 as
nuclear fusion d + t $\rightarrow He^{++}$ + n	17 MeV	$\sim 10^{-7}$ as.

Other time scales

Solids:
thermalization
relaxation of defects

Clusters:
ionization, electron detachment
Coulomb explosion of the positively charged cluster $\sim$ 100 fs

Attosecond physics is the physics of the dynamics of valence electrons

2.2 Photoionization

Multi-photon ionization

Wave length 800 nm, laser photon energy $\sim 1.5\,\mathrm{eV}$
Ionization potential (hydrogen) 13.6 eV
An electron needs to absorb at least 9 photons to leave the atom and reach the continuum.

Above threshold ionization

The electron absorbs many more photons than needed for escaping (and thus escapes with considerably larger velocity)!
"Above threshold ionization — ATI"

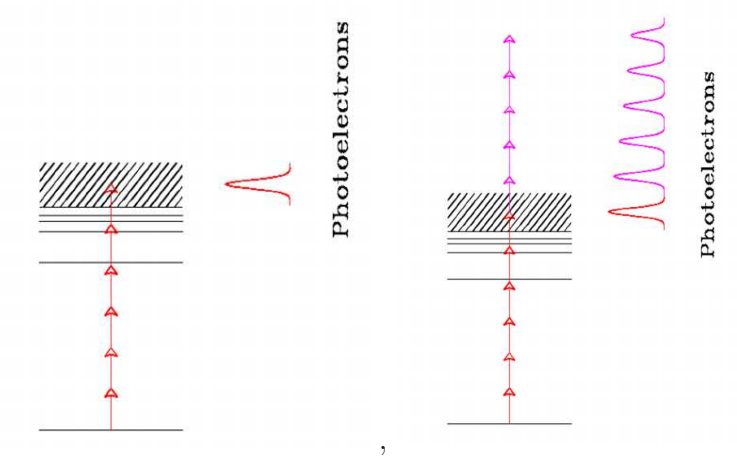

Figure 2.2: Multiphoton-ionization and above threshold ionization

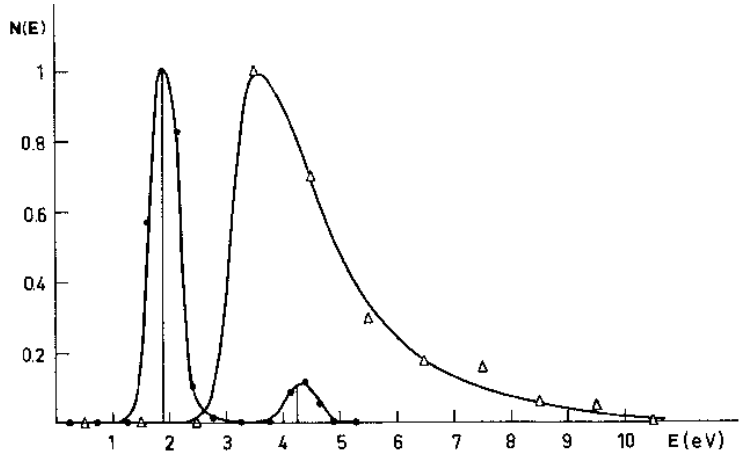

FIG. 3. Energy spectra of the emitted electrons for two photon energies: triangles, $\hbar\omega = 1.17$ eV, $I = 4\times10^{13}$ W/cm^{-2}, $E_{max} = 4$ eV; circles, $\hbar\omega = 2.34$ eV, $I = 8\times10^{12}$ W/cm^{-2}, $E_{max} = 0.2$ eV (E_{max} is the maximum energy gained in the field gradient). The solid straight lines at 1.90 and 4.25 eV have heights proportional to the values of $(d\sigma^{(m)}/d\Omega)$ $(d\sigma^{(el)}/d\Omega)^{-1}$ calculated from Eq. (3) using an intensity of 1.0×10^{13} W/cm^{-2}. The solid curves have been hand drawn through the experimental points.

Figure 2.3: Early experimental results on multi-photon ionization and ATI electrons. Photoelectrons from the lower $\hbar\omega$ and higher intensity appear at higher energies - "above threshold". From Agostini *et al., (1997)* [1]

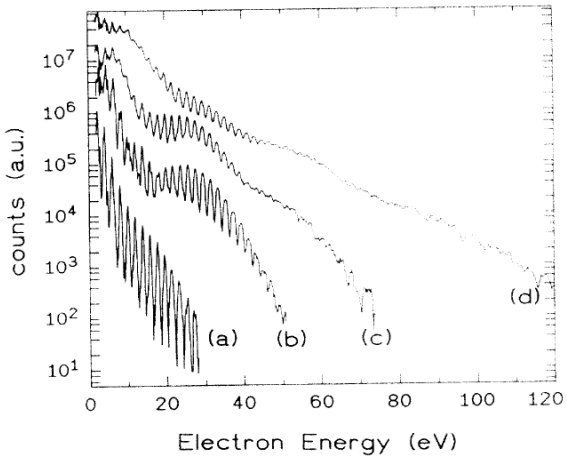

FIG. 2. ATI spectra from Ar with 40 fs, 630 nm pulses at intensities of 6×10^{13} W/cm^2 (*a*), 1.2×10^{14} W/cm^2 (*b*), 2.4×10^{14} W/cm^2 (*c*), and 4.4×10^{14} W/cm^2 (*d*) (the curves are separated slightly in the vertical direction for visual convenience).

Figure 2.4: Measured at MPQ, Paulus et al. 1993 [13]. Depending on intensity, cuttoffs and plateaus are visible.

Why and how? $\rightarrow$ to be explained later

Photo-ionization at extreme intensities

Some phenomenology: The 2 U_p and the 10 U_p cutoff.
Note: 2 U_p is the *maximum* kinetic energy of a *free* electron in a laser field (see below)
Where do the 10 U_p come from?

The ponderomotive potential U_p

We want to determine the mean energy of a (classical) electron in a plane wave electromagnetic field:

Continuous wave (cw) laser field

The electric field of a continuous, monochromatic wave with frequency ω is given by

$$\mathcal{E}(t) = \mathcal{E}_0 \cos \omega t. \tag{2.17}$$

Here dipole approximation is used, i.e. the field does not depend on space coordinates (which is a reasonable assumption as long as the wave length of the laser field is large compared to the atom).

Kinetic energy

With $v_e(0) = 0$ we find for the velocity of an electron in such a field

$$F = \dot{v}(t)m_e = -e\mathcal{E}(t) \Rightarrow v(t) = -\int_0^t \frac{e\mathcal{E}(t)}{m_e}dt = -\frac{e}{m_e}\frac{\mathcal{E}_0}{\omega}\sin\omega t. \tag{2.18}$$

With $e := 1,\ m_e := 1$ the kinetic energy of the electron at a time t is given by

$$T(t) = \frac{|v_e(t)|^2}{2} = \frac{\mathcal{E}_0^2}{2\omega^2}\sin^2\omega t. \tag{2.19}$$

This describes the "quiver motion" of the electron. The time averaged kinetic energy is

$$\langle T\rangle = \langle\frac{|v_e(t)|^2}{2}\rangle = \frac{\mathcal{E}_0^2}{4\omega^2} =: U_p\ . \tag{2.20}$$

From (2.19) we conclude that the maximum kinetic energy of an electron in a cw laser field is given by $2U_p$.

2.3 HHG — high harmonic generation

Traditional harmonic generation

Simple, instantaneous non-linear response of a medium to the laser:

$$\mathbf{P}(\mathcal{E}) = \chi^{(1)}\mathcal{E} + \chi^{(2)}\mathcal{E}\mathcal{E} + \chi^{(3)}\mathcal{E}\mathcal{E}\mathcal{E} + \dots \tag{2.21}$$

For an isotropic medium we have: $\chi^{(2n)} = 0$. This follows from $\mathbf{P}(\mathcal{E}) = -\mathbf{P}(-\mathcal{E})$.
Since the 'secondary' field generated by the medium is proportional to $\ddot{\mathbf{P}}$ and $\mathcal{E} \sim \cos\omega t,\ \mathcal{E}^2 \sim \cos^2\omega t \sim 1 + \cos 2\omega t,\ \mathcal{E}^3 \sim \cos^3\omega t \sim 3\cos\omega t + \cos 3\omega t \dots$, we see that only odd multiples are generated. We speak of *frequency tripling, quintupling, heptapling...* Only *odd* multiples of the fundamental frequency can arise.
BUT: usually, there is a rapid decrease of intensity with harmonic order

Microscopic reason: expect $\sim$ exponential decrease from perturbation theory

Measurements at high intensities:

NOTE: the "plateau" indicates that there may be a sudden short-time process hidden in the spectrum. For example, compare the Fourier transform of a rectangular series of spikes (assuming a flat phase).

$$\boxed{\text{Cutoff energy: } I_p + 3.17U_p}$$

I_p ... ionization potential of the (gas) medium
Why U_p again? Why 3.17? — see below

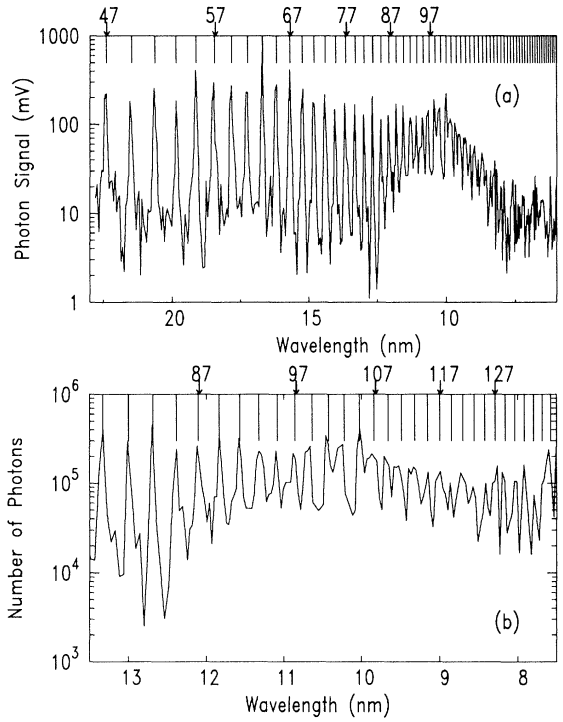

FIG. 2. Experimental spectrum obtained in neon at 40 Torr, 1.5 $\times 10^{15}$ W/cm^2. (a) Raw data; (b) data corrected from the spectrometer's response over 12–8 nm.

Figure 2.5: An early measurement of high harmonics [8]

2.4 Units and scaling

2.4.1 The time dependent Schrödinger equation

For a the hydrogen atom or a hydrogen-like ion (*i.e.* H, He^+, Li^{++},...) in an external electric field the time dependent Schrödinger equation is

$$i\hbar\frac{d}{dt}\Psi(\vec{r},t) = \left[-\frac{\hbar^2\Delta}{2m_e} - \frac{e^2}{4\pi\epsilon_0}\frac{Z}{r} - e\vec{\mathcal{E}}(t)\cdot\vec{r}\right]\Psi(\vec{r},t), \tag{2.22}$$

where Ze is the charge of the nucleus.

2.4.2 Atomic units

Set $\hbar = m_e = e = \frac{1}{4\pi\epsilon_0} = 1$, where e is the (positive) charge of the proton.

Unit	definition	numerical value
Length	$a_0 = \frac{(4\pi\epsilon_0)\hbar^2}{m_e e^2}$	0.052917 nm
Energy	2Ry $= \frac{e^2}{(4\pi\epsilon_0)a_0}$	27.211 eV
Velocity	$v_0 = \frac{e^2}{(4\pi\epsilon_0)\hbar c}$	$c/137.035$
Time	$\tau_0 = \frac{a_0}{v_0}$	24.188×10^{-18}s
Field strength	$\mathcal{E}_0 = \frac{e^2}{(4\pi\epsilon_0)a_0^2}$	5.1422×10^{11}V/m
Intensity	$I_0 = c\epsilon_0\mathcal{E}_0^2/2$	$3.50944\times10^{16}W/cm^2$
Wave-length @ 2Ry	$\frac{2\pi a_0}{\alpha}$	45.563 nm
Optical cycle @ 800 nm	$\frac{800nm}{c}$	110.32 au

Table 2.1: A few important quantities of laser-atom interactions and their relation to atomic units (au): $m_e = \hbar = e = 1$. Vacuum permittivity and speed of light are denoted by ϵ_0 and c, respectively.

2.4.3 Scaling of the Schrödinger equation

All hydrogen-like atoms are alike

Let us perform a substitution in the Schrödinger equation:

$$\vec{r} = \vec{u}/Z \qquad t = \tau/Z^2. \tag{2.23}$$

In atomic units the equation becomes:

$$iZ^2\frac{d}{d\tau}\Psi_Z(\vec{u}/Z,\tau/Z^2) = Z^2\left[-\frac{\Delta_u}{2} - \frac{1}{u} - \frac{1}{Z^3}\vec{\mathcal{E}}(\tau/Z^2)\cdot\vec{u}\right]\Psi_Z(\vec{u}/Z,\tau/Z^2). \tag{2.24}$$

Canceling Z^2 on both sides we recover the TDSE for hydrogen, but of course for a different electric field. (Ψ_{old} is the one in equation (2.22)),

$$\Psi_Z(\vec{u}/Z,\tau/Z^2) := \Psi_{old}(\vec{r},t) \Rightarrow \Psi_Z(\vec{r},t) = \Psi_{old}(Z\vec{r},Z^2t). \tag{2.25}$$

The wave function corresponding to a nuclear charge Z is smaller (factor $1/Z$) and faster evolving (factor Z^2) than a wave function corresponding to a nuclear charge $Z = 1$. It follows immediately, that the momentum/velocity increases with Z and the energy with Z^2. In order to get the same effects as for $Z = 1$, one must increase the field amplitude with a factor Z^3 (leading to an intensity growth of Z^6). Summary:

Scaling with nuclear charge Z

size of the wave function	shrinks	$\sim 1/Z$
momentum / velocity $\sim \vec{\nabla}$	grows	$\sim Z$
time	processes accelerate	$\sim Z^2$
energies	grow	$\sim Z^2$
electric fields	increase for same effect	$\sim Z^3$
laser intensities	increase for same effect	$\sim Z^6$

Chapter 3

Static field ionization

Given a constant external electric field $\vec{\mathcal{E}}_0$, the potential energy of the electron in the field is $V(\vec{r}) = -\vec{r}\cdot\vec{\mathcal{E}}_0$. The total Hamiltonian of an electron in a hydrogen atom with an applied external electric field is thus given by ($e = 1$):

$$H = -\frac{1}{2}\Delta - \frac{1}{r} - \vec{r}\cdot\vec{\mathcal{E}}_0. \tag{3.1}$$

3.1 A quick estimate

Gamov factor for a tunneling transition

$$\Gamma_{\text{tunnel}} \sim \exp\left[-2^{3/2}\int_0^{r_0}\sqrt{V(r)-E_0}\,dr\right], \tag{3.2}$$

$$r_0 : V(r_0) - E_0 = 0. \tag{3.3}$$

For a square well with a static field

$$V(r) = -\vec{r}\cdot\vec{\mathcal{E}}_0, \tag{3.4}$$

$$\int_0^{r_0}(\vec{r}\cdot\vec{\mathcal{E}}_0 - E_0)^{1/2}dr = \frac{2}{3}\frac{(-E_0)^{3/2}}{\mathcal{E}_0}, \tag{3.5}$$

$$\Rightarrow \Gamma_{\text{tunnel}} \propto \exp\left[-\frac{2}{3}\frac{(-2E_0)^{3/2}}{\mathcal{E}_0}\right].$$

Key features:

- exponential decrease with the binding potential E_0
- exponential decrease with $1/\mathcal{E}_0$, *i.e.* dramatic increase with $\mathcal{E}_0$.

3.2 A more accurate treatment

[This summary follows Landau-Lifshits, Quantum Mechanics, chap. X]

Construction of the model:

- use the exact field-free atomic wave function "inside" the atom
- use a quasi-classical solution "outside" the atom
- connect both solutions smoothly at some point under the tunneling barrier

Problem: There is a smooth connection needed in 3 dimensions. However, the *radius* where the potential barrier is highest or the radius at the "exit of the tunnel" depend on the spatal direction. Matching would be very difficult. Solution: use parabolic coordinates:

$$\eta = r + z, \qquad \xi = r - z, \qquad \xi, \eta \in [0, \infty). \tag{3.6}$$

Ground state eigenvalue equations in parabolic coordinates with an external field in z-direction $V(\vec{r}) = -\vec{r} \cdot \vec{\mathcal{E}}_0 = -z\mathcal{E}_0 = (\xi - \eta)\mathcal{E}_0/2$, with $\mathcal{E}_0 \ll 1$.

$$\begin{aligned} \Psi(x,y,z) &= \frac{1}{\sqrt{\xi\eta}}\phi(\xi)\chi(\eta) \Rightarrow \\ 0 &= \left[-\frac{\partial^2}{\partial\xi^2} - \frac{E_0}{2} - \frac{1}{2\xi} - \frac{1}{4\xi^2} + \frac{\mathcal{E}_0}{4}\xi\right]\phi(\xi), \\ 0 &= \left[-\frac{\partial^2}{\partial\eta^2} - \frac{E_0}{2} - \frac{1}{2\eta} - \frac{1}{4\eta^2} - \frac{\mathcal{E}_0}{4}\eta\right]\chi(\eta). \end{aligned}$$

- Since the potential barrier arises in the negative z-direction (thus in the direction of η), tunneling occurs mainly for large η and small ξ (*i.e.* $x \approx 0 \approx y$). Thus ϕ is little affected by the field (for $\mathcal{E}_0 > 0$) and may be assumed the same as in the field free case.
- χ as a function of only one variable can be pieced together easily.

For the field free case, the ground state hydrogen wave function in parabolic coordinates is given by

$$\psi = \frac{1}{\sqrt{\pi}} e^{-\frac{\xi+\eta}{2}}. \tag{3.7}$$

If we assume, in the case of an external field, that the exponential decaying shape of the wave function remains unchanged at some point η_0 *well inside the potential barrier*, with $1 \ll \eta_0 \ll 1/\mathcal{E}_0$. For $\chi(\eta)$ for some η outside the well we find

$$\chi = \left(\frac{\eta_0|p_0|}{\pi p}\right)^{1/2} \exp\left(-\frac{\xi+\eta_0}{2} + i\int_{\eta_0}^{\eta} p(\eta)d\eta + \frac{i\pi}{4}\right), \tag{3.8}$$

with

$$p(\eta) = \sqrt{-\frac{1}{4} + \frac{1}{2\eta} + \frac{1}{4\eta^2} + \frac{\mathcal{E}_0\eta}{4}} \tag{3.9}$$

(for p_0 see below). The phase factor $i\pi/4$ results from the patching of wave functions at the returning point η_1 (the point where the kinetic energy of the electron is zero at the outer 'margin' of the barrier). Since we are interested only in $|\chi|^2$, we may neglect the imaginary parts in the exponential functions. As the momentum p is imaginary inside the potential barrier, we remain with ($p(\eta_1) = 0$)

$$|\chi|^2 = \frac{\eta_0|p_0|}{\pi p} \exp\left(-\xi - 2\int_{\eta_0}^{\eta_1} |p| d\eta - \eta_0\right). \tag{3.10}$$

With $\eta \gg 1$, which is under the barrier if $\mathcal{E}_0$ is small, we may simplify the momenta in the pre-factor:

$$|p_0| \approx \frac{1}{2}, \qquad p \approx \frac{1}{2}\sqrt{\mathcal{E}_0\eta - 1}.$$

In the exponent we expand the momentum one term further and obtain

$$|\chi|^2 = \frac{\eta_0}{\pi\sqrt{\mathcal{E}_0\eta - 1}} \exp\left(-\xi - \int_{\eta_0}^{\eta_1} \sqrt{1 - \mathcal{E}_0\eta} d\eta + \int_{\eta_0}^{\eta_1} \frac{d\eta}{\sqrt{1 - \mathcal{E}_0\eta} - \eta_0}\right). \tag{3.11}$$

where we approximated $\eta_1 = 1/\mathcal{E}_0$, After integration and neglecting $\eta_0\mathcal{E}_0$ with respect to 1 we obtain

$$|\chi|^2 = \frac{4}{\pi\mathcal{E}_0\sqrt{\mathcal{E}_0\eta - 1}} \exp\left(-\xi - \frac{2}{3\mathcal{E}_0}\right). \tag{3.12}$$

Calculating the rate

We calculate the ionization rate as the *current* through a surface perpendicular to the field direction z (ionization happens only along the direction parallel to the field).
The electron density at a surface $z = z_0$ is: $|\Psi(x, y, z_0)|^2$.
We estimate the electron velocity at z_0 from the (classical) energy:

$$-0.5 \text{ a.u.} = E = \vec{v}^2/2 - z_0\mathcal{E}_0 \approx v_z^2/2 - z_0\mathcal{E}_0. \Rightarrow v_z \approx \sqrt{2z_0\mathcal{E}_0 - 1} \approx \sqrt{\eta\mathcal{E}_0 - 1},$$

since $z = \frac{1}{2}(\xi - \eta)$, $\xi \approx 0$ ($r \approx z, x^2 + y^2 \approx 0$). The perpendicular components $v_x = v_y \approx 0$ for reasons of cylindrical symmetry. The total current is given by the integration of the "current density" = "(charge) density × velocity",

$$\Gamma_{\text{tunnel}} = \int dx\, dy\, |\Psi(x, y, z_0)|^2 v_z = \int_0^\infty |\psi|^2 v_z 2\pi\rho d\rho$$

For large η ands small σ we have

$$d\rho = d\sqrt{\xi\eta} \approx \frac{1}{2}\sqrt{\frac{\eta}{\xi}}d\xi.$$

Thus the integral is

$$\Gamma_{\text{tunnel}} = \int_0^\infty |\xi|^2 \pi \sqrt{\mathcal{E}_0 - 1}\, d\xi.$$

For the hydrogen atom we find

$$\Gamma_{\text{tunnel}} = \frac{4}{\mathcal{E}_0} \exp\left(-\frac{2}{3\mathcal{E}_0}\right).$$

Scaling with nuclear charge

With the proper transformation of units we have The rate *increases* $\sim Z^2$, but the effect of the field *decreases* $\sim Z^{-3}$, (see discussion of the scaling above):

$$\begin{aligned} [\text{rate}] = [1/\text{time}] &\sim Z^2, \\ \mathcal{E}_0 &\sim Z^3, \end{aligned}$$

$$\Gamma_{\text{tunnel}}(\mathcal{E}_0, Z) Z^2 \Gamma(\mathcal{E}_0/Z^3, 1) = Z^5 \frac{4}{\mathcal{E}_0} \exp\left(-\frac{2Z^3}{3\mathcal{E}_0}\right).$$

Note: Since the exponential function 'kills' the polynomial, for $\mathcal{E}_0$=const, there is a dramatic *decrease* of the ionization rate with increasing Z.

3.3 Numerical confirmations of the tunnel formula

There exist several methods:

1 Solve the time-dependent Schrödinger equation (TDSE)

$$i\frac{\partial}{\partial t}\Psi(\vec{r}, t) = \left[-\frac{1}{2}\Delta - \frac{1}{r} - z\mathcal{E}_0\right]\Psi(\vec{r}, t)$$

Problem:
- there is no strictly exponential decay in quantum mechanics (at start time, because of time reversal symmetry;
For the mathematically inclined: for semi-bounded Hamiltonians there is also not exponential decay at time$\to \infty$. However, our Hamiltonian is not semi-bounded.
- hard to do numerically
Advantage:
+ well defined procedure on the foundations of quantum mechanics

2 High order perturbation theory

Problem: it diverges! (Make convergent using obscure tricks: Pade or Borel-summation) Advantage: for hydrogen, it can be done analytically to very high (e.g. 18!) orders of perturbation theory.

3 Complex scaling

Analytically continue the Hamiltonian to *complex coordinates!*

$$\vec{r} \to e^{i\theta}\vec{r}$$

Find *complex* eigenvalues of

$$\left[-e^{-2i\theta}\frac{1}{2}\Delta - e^{-i\theta}\frac{1}{r} - e^{i\theta}z\mathcal{E}_0\right]\Psi(\vec{r}) = (E - \frac{i}{2}\Gamma_{\text{tunnel}})\Psi(\vec{r})$$

The imaginary part of a given eigenvalue is *half the tunnel rate* for the corresponding state: $\frac{1}{2}\Gamma_{\text{tunnel}}$.

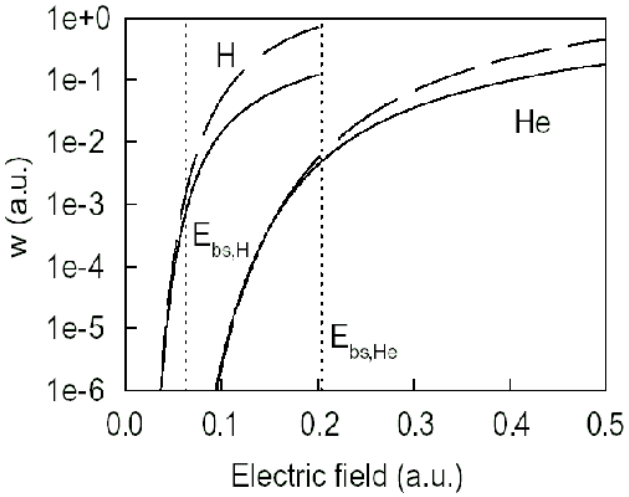

Figure 3.1: ADK vs. numerically accurate static field ionization rates.

At present, there are no strong static field ionization rates available for other system. A numerical check of the CW ionization rates at 800 nm for other systems shows *very severe* discrepancies [16].

3.4 The Ammosov-Delone-Krainov (ADK) formula

Based on the same ideas of stitching together the field-free atomic state with WKB-like solutions at some point "under the tunnel barrier", a more general formula for field

ionization of atoms was derived in 1966 by Perelomov, Popov and Terentev [14] and later in by Ammosov, Delone, Krainov [2]. These formula come in many variants and promise to be applicable to all kinds of atoms in all kinds of states. In most cases, a verification is not available to the present day. The formulae are deliberately not quoted here. They all are accurate "to exponential accuracy", i.e. the exponential dependence on field and binding energy is reproduced correctly (but near trivially). This is the use that is made of them in practice.

3.4.1 Molecular ADK

The ADK formula was further generalized by X.M.Tong et al. [Phys. Rev. A 66, 033402 (2002)] using an intriguingly simple idea: assume that the tunnel barrier reaches its maximum at somewhat larger distances from the molecule (moderate fields). Again, we would like to smoothly connect a WKB solution to the wave function under the barrier, which is assumed to coincide with the field-free solution. Expand the field-free solution (known from some quantum chemistry calculation) into atom-like expansion functions and use the only the dominant ones to to the WKB solution.

Chapter 4

Above threshold ionization (ATI)

4.1 Initial velocity after tunneling

At the end of the tunnel, we have total energy = potential energy

$$E_0 = V(r_0) = -\frac{1}{r_0} - r_0\mathcal{E}_0,$$

therefore we expect the kinetic energy to be ~ 0.

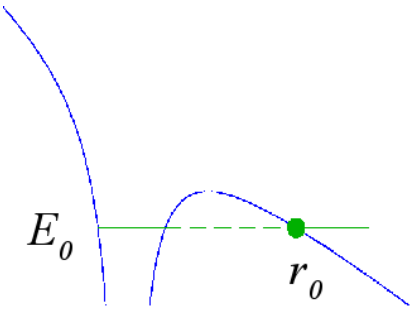

Figure 4.1: Potential of a Coulomb-system with an external static field.

Velocity perpendicular to the field

$v_\perp \sim 0$ because of symmetry reasons.

Quantum version of this idea

Energy in perpendicular direction:

$$-\frac{\partial^2}{\partial x^2}\Psi(x,y,z) = -\frac{\partial^2}{\partial y^2}\Psi(x,y,z) \sim 0,$$

$$\frac{1}{2}\frac{\partial^2}{\partial z^2}\Psi(x,y,z) \sim \frac{1}{2}\Delta\Psi|_{r_0} = \left(-\frac{1}{r} - r\mathcal{E}_0 - E_0\right)\Psi|_{r_0} = 0. \tag{4.1}$$

The electron emerges from tunneling with velocity = 0

4.1.1 Remark

There is some cheating: due to the uncertainty relation,

$$\Delta p_z \Delta z \geq \frac{\hbar}{2}, \qquad \Delta E \Delta t \geq \frac{\hbar}{2},$$

there is no such thing as a "velocity v_z at a point z_0. Similarly, there is no such thing as a "time when the electron leaves the barrier".

The idea is difficult to make precise, but seems to be qualitatively correct.

4.2 ATI - above threshold ionization

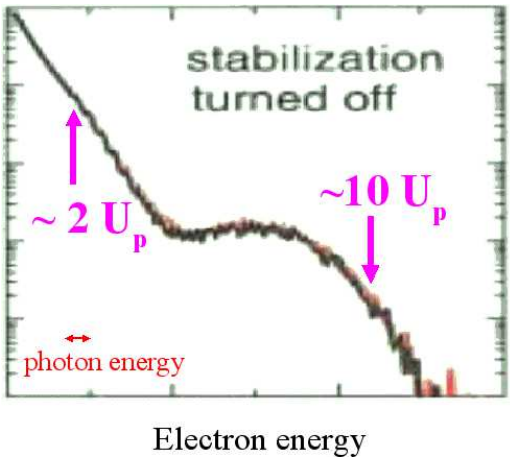

Figure 4.2: Photoelectron spectrum generated by a 5fs laser pulse. A large number of photons is absorbed, maximal electron energies widely exceed the photon energy. The distinct structure is characterized by two the values of $2U_p$ and $10U_p$. (From Ref. [12])

4.2.1 Quasi-static, classical picture

Acceleration of an electron in a laser field (after tunneling)

(remember atomic units, $e^2/4\pi\varepsilon_0 = 1$, electron charge e is negative, $m_e = 1 \Rightarrow \vec{p} = \dot{\vec{r}}$)

$$\begin{aligned} \ddot{\vec{r}}(t) &= -\vec{\mathcal{E}}(t), \\ \dot{\vec{r}}(t) = \vec{p}(t) &= -\int_{t_0}^{t} \vec{\mathcal{E}}(t')dt' =: \vec{A}(t) - \vec{A}(t_0) + v(t_0). \end{aligned}$$

Here we have defined the

Vector potential $\vec{A}(t)$

$$\vec{A}(t) = -\int_{-\infty}^{t} \mathcal{E}(t')\, dt'. \tag{4.2}$$

Note: Compared to the usual definition of the vector potential (in Coulomb gauge) we have absorbed a factor $\frac{e}{c}$ into $\vec{A}$.

As a laser pulse cannot have a dc component in its spectrum we see that

$$0 = -\int_{-\infty}^{\infty} dt e^{i\omega t}\mathcal{E}(t)\Big|_{\omega=0} = \vec{A}(\infty) - \vec{A}(-\infty). \tag{4.3}$$

The value of $\vec{A}$ at infinity can be set $\equiv 0$ without loss of generality

$$A(t = \infty) = A(t = -\infty) := 0 \tag{4.4}$$

Note: any (laser-)pulse shape must fulfill this condition

Initial and final electron momenta

Initial (at the end of the tunnel): $v(t_0) = 0 \Rightarrow p(t_0) = 0$.
With an electron release time t_0:

$$\vec{p}(t = \infty) = -\vec{A}(t_0).$$

The vector potential gives the acceleration of an electron in the field

4.2.2 Crossection $\sigma(p)$ for electrons with final momentum p

Since there exists a clear relation between the release time of an electron and its momentum, we may assume:

$$\sigma(p)dp = \sigma(p)\frac{dp}{dt}dt = \sigma(p)\mathcal{E}(t)dt := w(t)dt$$

Quasi-static ionization rate

$$w(t) = \frac{4}{\mathcal{E}(t)} e^{-\frac{2}{3\mathcal{E}(t)}} \tag{4.5}$$

$$\sigma(p)\mathcal{E}(t)dt = w(t)dt$$

$$\sigma(p) = \frac{4}{\mathcal{E}(t)^2} e^{-\frac{2}{3}\frac{1}{\mathcal{E}(t)}}$$

In spite of the singularity, because of the exponential, this functions rapidly drops to zero where $\mathcal{E}(t) = 0$.

$$\mathcal{E}(t) = \mathcal{E}_0 \cos(\omega t), \quad p(t) = -\int_t^\infty \mathcal{E}(t')dt' \;\Rightarrow$$

$$p(t) = \mathcal{E}_0/\omega \sin(\omega t), \quad t(p) = \arcsin\left(\frac{p\omega}{\mathcal{E}_0}\right),$$

$$\mathcal{E}(p) = \mathcal{E}_0\sqrt{1 - p^2/A_0^2}$$

$$\boxed{\sigma(p) = \frac{4}{\mathcal{E}_0(1 - (p/A_0)^2)} e^{-\frac{2}{3}\frac{1}{\mathcal{E}_0[1-(p/A_0)^2]}}} \tag{4.6}$$

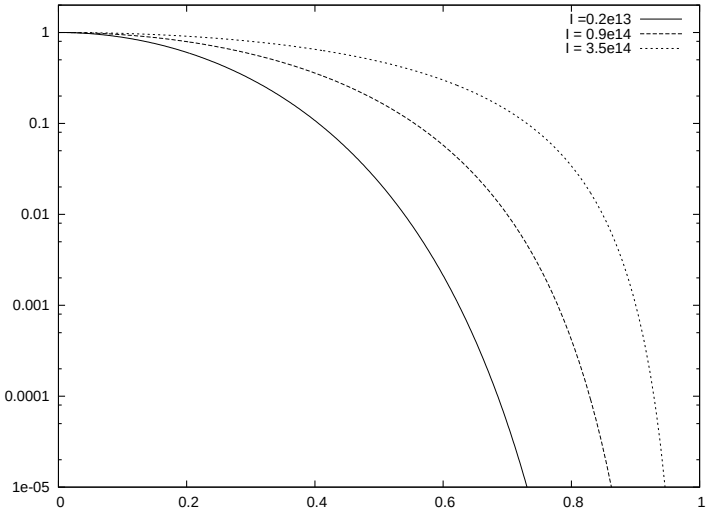

Figure 4.3: The classical ionization according to Eq. 4.6

Maximal acceleration from times where $\mathcal{E}(t) = 0$

For a cw laser field we find

$$p_{\max} = \mathcal{E}_0/\omega := A_0, \tag{4.7}$$

$$\frac{p_{\max}^2}{2} = \frac{\mathcal{E}_0^2}{2\omega^2} := \frac{A_0^2}{2} = 2U_p. \tag{4.8}$$

4.3 The 10 U_p cutoff

Re-scattered ATI electrons

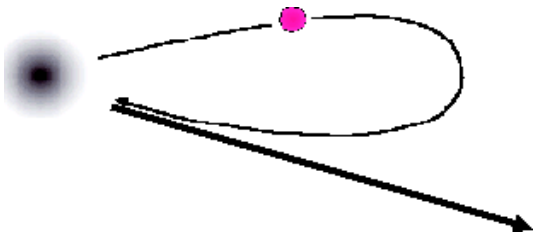

Figure 4.4: An electron is removed from an atom, returns to the atom and re-collides.

The electron must return to its initial position

Ionization at t_0, rescattering at t_1

$$z(t_1) - z(t_0) = \int_{t_0}^{t_1} \underbrace{\left(- \int_{t_0}^{t} \mathcal{E}(t')dt' \right)}_{v(t)} dt = 0. \tag{4.9}$$

For a cw laser field $\mathcal{E}(t) = \mathcal{E}_0 \cos(\omega t)$ we find

$$v(t) = -\frac{\mathcal{E}_0}{\omega}(\sin(\omega t) - \sin(\omega t_0)). \tag{4.10}$$

With this, condition (4.9) becomes

$$0 = \frac{\mathcal{E}_0}{\omega^2}[\cos(\omega t_1) - \cos(\omega t_0)] + \frac{\mathcal{E}_0}{\omega}\sin(\omega t_0)(t_1 - t_0). \tag{4.11}$$

This is a transcendental equation, which can be solved graphically or numerically.

The graphical solution is represented as follows:

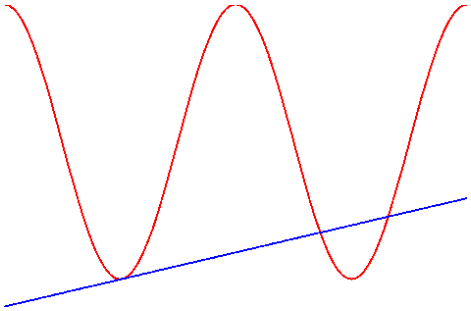

Figure 4.5: Graphical solution of Eq. (4.11). The red (wavy) line represents the first term in (4.11), the blue (straight) line the second term. The slope of the straight line is equal to the derivative of the wave at t_0, i.e. the straight line is the tangent at to the wave at t_0. Where it intersects the wave, the offsets produced by the two terms are equal with opposite sign and therefore cancel

Total acceleration

From t_0 to t_1 = momentum at t_1: $p(t_0, t_1) := \int_{t_0}^{t_1}[-\mathcal{E}(t)]dt = A(t_1) - A(t_0)$.

From t_1 to the end of the pulse: $p(t_1, \infty) = \int_{t_1}^{\infty}[-\mathcal{E}(t)]dt = -A(t_1)$.

If the electron does NOT scatter at t_1, the final momentum is simply $A(t_0)$:

$$p_{final}(t_0) = p(t_0, t_1) + p(t_1, t_\infty) = -A(t_0)$$

If the electron DOES scatter elastically at t_1, the momentum may change direction at time t_0. E.g., the momentum acquired between t_0 and t_1 may reverse sign: $p(t_0, t_1) \to -p(t_0, t_1)$.
In that case the final momentum is

$$p_{final}(t_0) = -p(t_0, t_1) + p(t_1, t_\infty) = -2A(t_1) + A(t_0)\,.$$

Depending on the release time t_0, the maximal final momentum with rescattering is thus

$$p_{\max} = \max(t_0)|-2A(t_1) + A(t_0)|\,, \tag{4.12}$$

where t_0 and t_1 are related by the condition (4.9).

Numerical solution

$$\frac{p_{\max}^2}{2} = 10\,U_p\,.$$

NOTE: the numerical result very nearly 10 ($\sim$ 5 digits). This, however, seems to be a coincidence, as there remains a deviation after the 4th digit.

Chapter 5

Quantum mechanical description

5.1 Length- and velocity gauge

The Schrödinger equation in "length gauge"

$$i\frac{d}{dt}\Psi_L(\vec{r},t) = \left[-\frac{1}{2}\Delta - \frac{1}{r} - \vec{r}\cdot\vec{\mathcal{E}}(t)\right]\Psi_L(\vec{r},t) \tag{5.1}$$

can be brought to a different form by a gauge transformation

$$\Psi_L(\vec{r},t) = e^{-i\vec{A}\cdot\vec{r}}\Psi_V(\vec{r},t), \tag{5.2}$$

with the vector potential

$$\vec{A}(t) = -\int_{-\infty}^{t}\vec{\mathcal{E}}(t')dt', \qquad \vec{\mathcal{E}}(t) = -\frac{d}{dt}\vec{A}(t) \tag{5.3}$$

Inserting the ansatz (5.2) into (5.1) we find the **TDSE in the "velocity gauge"**

$$i\frac{d}{dt}\Psi_V(\vec{r}) = \left[\frac{1}{2}\left(-i\vec{\nabla} - \vec{A}(t)\right)^2 - \frac{1}{r}\right]\Psi_V(\vec{r}). \tag{5.4}$$

Note 1

the physical meaning of $-i\vec{\nabla}$ differs in the two gauges:
length gauge: $-i\vec{\nabla}/m_e \sim$ velocity $\dot{\vec{r}}$
velocity gauge: $-i\vec{\nabla}/m_e \sim \dot{\vec{r}} + \vec{A}(t)/m_e$

Note 2

the *field free* hydrogen ground state function Φ takes different forms in the two gauges:
length gauge: $\Phi_L(\vec{r}) \sim e^{-r}$, i.e. unchanged
velocity gauge: $\Phi_V(\vec{r}) = e^{i\vec{A}\cdot\vec{r}}\Phi_L(\vec{r})$ i.e. multiplied by a $\vec{r}$-dependent phase = shifted in Fourier-space

Note 3

The term $\sim \vec{A}(t)^2$ in Eq. (5.4) is often omitted, as it only leads to an additional time-dependent, but space-independent phase $\exp\left[-i\int_{-\infty}^{t}\vec{A}^2(t')dt'\Big/2\right]$ on the wave function with no effect on observables.

5.2 Volkov solutions

We determine the solution of the TDSE of a free electron in presence of a dipole (laser) field. For this we use the velocity gauge form of the TDSE:

$$i\frac{d}{dt}\chi(\vec{r},t) = \frac{1}{2}\left[-i\vec{\nabla} - \vec{A}(t)\right]^2\chi(\vec{r},t). \tag{5.5}$$

We perform a spatial Fourier transform

$$\chi(\vec{r},t) = \frac{1}{(2\pi)^{3/2}}\int d\vec{k}e^{i\vec{k}\cdot\vec{r}}\tilde{\chi}(\vec{k},t), \tag{5.6}$$

$$i\frac{d}{dt}\tilde{\chi}(\vec{k}) = \frac{1}{2}\left[\vec{k} - \vec{A}(t)\right]^2\tilde{\chi}(\vec{k}), \tag{5.7}$$

$$\tilde{\chi}(\vec{k},t) = \tilde{\chi}(\vec{k},0)\,e^{-i\int_0^t\frac{1}{2}[\vec{k}-\vec{A}(\tau)]^2d\tau}. \tag{5.8}$$

Inverse Fourier transform

$$\chi(\vec{r},t) = \frac{1}{(2\pi)^{3/2}}\int d\vec{k}e^{i\vec{k}\cdot\vec{r}}\tilde{\chi}(\vec{k},t) \tag{5.9}$$

$$= \frac{1}{(2\pi)^{3/2}}\int d\vec{k}\,\underbrace{e^{i\vec{k}\cdot\vec{r}}e^{-i\int_0^t\frac{1}{2}[\vec{k}-\vec{A}(\tau)]^2d\tau}}\tilde{\chi}(\vec{k},0). \tag{5.10}$$

The underbraced term part (up to an unimportant time-independent phase $\Phi(\vec{k},0)$) is the

Volkov solution in velocity gauge

$$|\vec{k}\rangle_V := \frac{1}{(2\pi)^{3/2}}e^{i\vec{k}\cdot\vec{r}}e^{-i\Phi(\vec{k},t)}, \tag{5.11}$$

where we have defined the

Volkov phase $\Phi(\vec{k},t)$

$$\Phi(\vec{k},t) = \int_0^t\frac{1}{2}[\vec{k} - \vec{A}(\tau)]^2d\tau. \tag{5.12}$$

Volkov solution in length gauge

$$|\vec{k}\rangle_L := e^{-i\vec{A}\cdot\vec{r}}|\vec{k}\rangle_V = \frac{1}{(2\pi)^{3/2}} e^{i(\vec{k}-\vec{A})\cdot\vec{r}} e^{-i\Phi(\vec{k},t)}. \tag{5.13}$$

5.3 Quantum mechanics of laser-atom interaction

Our physical picture so far

- "inside" the atom the electrons are little affected by the laser field and remain close to the *field free* ground state
- "outside" the atom the electrons are nearly free

Ansatz for the solution of the TDSE

$$|\Psi(\vec{r},t)\rangle = c(t)\underbrace{|0,t\rangle}_{\text{inside}} + \underbrace{\int d\vec{k}\, b(\vec{k},t)\,|\vec{k},t\rangle_L}_{\text{outside}}, \tag{5.14}$$

where $|0,t\rangle$ solves the TDSE without a laser field,

$$i\frac{d}{dt}|0,t\rangle = \left[-\frac{\Delta}{2} + V(\vec{r})\right]|0,t\rangle, \tag{5.15}$$

and $|\vec{k},t\rangle$ are Volkov solutions. Here a general atomic binding potential is assumed. In case of hydrogen $V(\vec{r}) = -\frac{1}{r}$.

Is the ansatz complete?

Yes! The Volkov solutions form a complete set of functions (this is related to the fact that the Fourier transform is complete in L^2)

Why do we need $c(t)|0,t\rangle$?

We want to describe the electrons "inside" by the field free ground state.

Problem

The ansatz is *over*-complete, i.e. we can express $|0,t\rangle$ as a linear combination of $|\vec{k},t\rangle$.

Additional condition

needed to obtain a unique solution for $c(t)$ and $b(\vec{k},t)$:

$$\langle 0,t|\left[\int d\vec{k} b(\vec{k},t)|\vec{k},t\rangle\right] = 0, \tag{5.16}$$

i.e. we want no content of the ground state in the part of the free wave packet.

5.3.1 Equations for $c(t)$ and $b(\vec{k},t)$

We have the ansatz

$$\Psi = c(t)|0\rangle + b_k(t)|k\rangle \tag{5.17}$$

with the constraint

$$\langle 0|k\rangle b_k = 0. \tag{5.18}$$

For convenience we use the short hand notation $b_k = b(\vec{k},t)$ and we employ the "summenkonvention" with respect to k, which means that integrations over k are assumed where it appears twice in a product. The full Hamiltonian operator of our system can be split in two different ways as

$$H = H_0 + F = H_F + V. \tag{5.19}$$

The expansion vectors are defined by the properties

$$i\partial_t|0\rangle = H_0|0\rangle = E_0|0\rangle \tag{5.20}$$
$$i\partial_t|k\rangle = H_F|k\rangle. \tag{5.21}$$

We now use a variational principle to derive the Schrödinger equation in terms of the expansion coefficients $c(t)$ and $b_k(t)$. We write the Dirac-Frenkel variational principle

$$0 = \langle \delta\Psi^*|i\partial_t - H|\Psi\rangle \tag{5.22}$$

in terms of variations of the expansion coefficients

$$\langle\delta\Psi| = \delta c^*\langle 0| + \delta b^*_{k'}\langle k'|.$$

The orthogonality constraint $b^*_{k'}\langle k'|0\rangle$ is taken into account by a Lagrange multiplier λ, which leads to the variational equation

$$0 = \delta c^*\langle 0|\left[i\partial_t - H|\Psi\rangle\right] + \delta b^*_{k'}\langle k'|\left[i\partial_t - H|\Psi\rangle\right] + \lambda\delta b^*_{k'}\langle k'|0\rangle. \tag{5.23}$$

We next separate the equations for the individual variations. For the δc^* variation we have

$$\begin{aligned}
0 &= \langle 0|\left[i\partial_t - H|\Psi\rangle\right] \\
&= \langle 0|\left[i\partial_t - H_0 - F|0\rangle c(t)\right] + \langle 0|\left[i\partial_t - H_F - V|k\rangle b_k(t)\right] \\
&= -\langle 0|F|0\rangle c(t) + \langle 0|0\rangle i\partial_t c(t) - \langle 0|V|k\rangle b_k(t) + \langle 0|k\rangle i\partial_t b_k(t) \\
&= i\partial_t c(t) - \langle 0|V|k\rangle b_k(t) + \langle 0|k\rangle i\partial_t b_k(t)
\end{aligned}$$

where we have used (5.20) and (5.21). For simplicity, we further assumed that $|0\rangle$ has no expectation value for the field. This is the case, e.g., if the interaction is dipole and the ground state has no dipole moment $\langle 0|F|0\rangle = 0$.

For the $\delta b^*_{k'}$ variation we obtain

$$\begin{aligned} 0 &= \langle k'|\left[i\partial_t - H|\Psi\rangle\right] + \langle k'|0\rangle\lambda \\ &= \langle k'|\left[i\partial_t - H_0 - F|0\rangle c(t)\right] + \langle k'|\left[i\partial_t - H_F - V|k\rangle b_k(t)\right] + \langle k'|0\rangle\lambda \\ &= -\langle k'|F|0\rangle c(t) + \langle k'|0\rangle i\partial_t c(t) - \langle k'|V|k\rangle b_k(t) + \langle k'|k\rangle i\partial_t b_k(t) + \langle k'|0\rangle\lambda \end{aligned}$$

With this we obtain the equations for the coefficients

$$i\partial_t c = \langle 0|V|k\rangle b_k - \langle 0|k\rangle i\partial_t b_k \tag{5.24}$$

$$i\partial_t b_k = \langle k|F|0\rangle c + \langle k|V|k'\rangle b_{k'} - \langle k|0\rangle i\partial_t c - \lambda\langle k|0\rangle + \langle k'|0\rangle\lambda, \tag{5.25}$$

where we have assumed a δ-normalization of the Volkov functions $\langle k'|k\rangle = \delta(k-k')$. Now we use the derivative form of the constraint

$$0 = i\partial_t\langle 0|k\rangle b_k = -E_0\underbrace{\langle 0|k\rangle b_k}_{=0} + \langle 0|H_F|k\rangle b_k + \langle 0|k\rangle i\partial_t b_k \tag{5.26}$$

to replace the derivative of b_k in (5.24) and substitute (5.27) into (5.25):

$$i\partial_t c = \langle 0|V|k\rangle b_k + \langle 0|H_F|k\rangle b_k = E_0\underbrace{\langle 0|k'\rangle b_{k'}}_{=0} + \langle 0|F|k'\rangle b_{k'} \tag{5.27}$$

$$i\partial_t b_k = \langle k|F|0\rangle c + \langle k|V|k'\rangle b_{k'} - \langle k|0\rangle\langle 0|F|k'\rangle b_{k'} - \langle k|0\rangle\lambda \tag{5.28}$$

The Lagrange multiplier λ is determined from substituting (5.28) into (5.26) which gives

$$\lambda = \langle 0|H_F|k'\rangle b_{k'} + \langle 0|V|k'\rangle b_{k'} - \langle 0|F|k'\rangle b_{k'}$$

where we have used the completeness of the Volkov functions $|k'\rangle\langle k| = 1$ and $\langle 0|F|0\rangle = 0$. Further one finds

$$\begin{aligned} \lambda &= \langle 0|H_F + V|k'\rangle b_{k'} - \langle 0|F|k'\rangle b_{k'} \\ &= \langle 0|H_0 + F|k'\rangle b_{k'} - \langle 0|F|k'\rangle b_{k'} \\ &= \langle 0|E_0 + F|k'\rangle b_{k'} - \langle 0|F|k'\rangle b_{k'} \\ &= E_0\underbrace{\langle 0|k'\rangle b_{k'}}_{=0} + \langle 0|F|k'\rangle b_{k'} - \langle 0|F|k'\rangle b_{k'} = 0 \end{aligned}$$

With $\lambda = 0$ in (5.28) we obtain the final form of the Schrödinger equation in terms of $c(t)$ and $b_k(t)$:

$$i\partial_t c = \langle 0|F|k'\rangle b_{k'} \tag{5.29}$$

$$i\partial_t b_k = \langle k|F|0\rangle c + \langle k|0\rangle\langle 0|H_F|k'\rangle b'_k + \langle k|V_\perp|k'\rangle b_{k'}, \tag{5.30}$$

where we have defined

$$V_\perp := [1 - |0\rangle\langle 0|]V[1 - |0\rangle\langle 0|]. \tag{5.31}$$

Note: NO approximations have been made, only the TDSE has been written in terms of $c(t)$ and $|b)$.

The individual terms in (5.29) and (5.30) have simple physical interpretations and can be given more explicitly for the hydrogen atom with the dipole approximation for the external field:

$V_\perp$ is the restriction of the atomic potential to the space orthogonal to $|0\rangle$: $\langle a|V_\perp|0\rangle = 0\,\forall|a\rangle$.

$\langle k|0\rangle$ is the initial state expressed in terms of Volkov functions. In case of Hydrogen with $|0,t\rangle \propto e^{-iE_0t}e^{-r}$:

$$\langle k|0\rangle = \frac{\sqrt{8}}{\pi}e^{i\Phi(\vec{k},t)-itE_0}\frac{1}{[1+(\vec{k}-\vec{A}(t))^2]^2}. \tag{5.32}$$

$\langle 0|F|k'\rangle$ is the interaction with the field, which moves amplitude between the bound state $|0\rangle$ and the continuum Volkov functions $|k\rangle$. For a dipole field $F = -\vec{r}\cdot\vec{\mathcal{E}}(t)$

$$-\vec{\mathcal{E}}(t)\cdot\underbrace{\langle\vec{k},t|\vec{r}|0,t\rangle}_{\text{dipole matrixelement}} \quad . \tag{5.33}$$

In the case of hydrogen this is given by

$$\langle\vec{k},t|\vec{r}|0,t\rangle = 4i\frac{\vec{\mathcal{E}}\cdot(\vec{k}-\vec{A})}{[1+(\vec{k}-\vec{A}(t))^2]}\langle\vec{k},t|0,t\rangle. \tag{5.34}$$

$\langle 0|H_F|k\rangle b_k$ appears, because $|k\rangle$ and $|0\rangle$ are not solutions of the same Schrödinger equation. It can be rewritten as

$$\langle 0|H_F|k\rangle b_k = \langle 0|F-V|k\rangle b_k. \tag{5.35}$$

In the usual derivation of the Lewenstein model this is referred to as the "Volkov functions are not orthogonal to the atomic ground state".

"But the Schrödinger equation is useless"

(famous quote by Vladimir Pavlovich Krainov)

Approximations

(1) The ground state is not depleted much $c(t) \approx 1$, $\dot{c}(t) \approx 0$.

(2) neglect the fact, that Volkov functions are not orthogonal to the ground state $\Leftrightarrow \langle 0|H_F|k\rangle b_k \approx 0$.

(3) set $V_\perp \approx 0$: **serious approximation!!**

Mostly approximation (3) is responsible for incorrect (tunnel-) ionization rates by the approximate theory. Rates are usually too low by roughly 1 order of magnitude (at low laser frequencies). The situation is better at higher frequencies.

Simplified form of the equation

$$\boxed{i\frac{\partial}{\partial t}b(\vec{k},t) = \langle \vec{k},t|F|0,t\rangle}$$

This can be easily integrated

"Strong field approximation (SFA)", "Lewenstein model"

$$\boxed{b(\vec{k},t) = \int_{-\infty}^{t} dt' e^{i\Phi(\vec{k},t')-iE_0t'}\vec{\mathcal{E}}(t')\cdot\vec{d}[\vec{k}-\vec{A}(t')].} \tag{5.36}$$

Here $\vec{d}[\vec{k}-\vec{A}(t')]$ is given by

$$\vec{d}[\vec{k}-\vec{A}(t')] = \langle \vec{k}, t=0|\ \vec{r}\ |\, 0, t=0\rangle, \tag{5.37}$$

and the phase factors in (5.36) stem from the time propagation of $\langle\vec{k},t|$ and $|0,t\rangle$, respectively.

It is useful to think about the meaning of this integral. At any time t' electron amplitudes in a range of momenta is put into the continuum according to the distribution given by $\vec{d}[\vec{k}-\vec{A}(t')]$. They then time-evolve like free electrons. The coherent! superposition of the electron amplitudes emitted at all times is what determines the final electron amplitude as a function and observed electron spectrum.

5.3.2 Computation of the dipole matrix element

Given the hydrogen ground state

$$|0\rangle = \sqrt{\frac{1}{\pi}}e^{-r} \tag{5.38}$$

and δ-normalized plane waves

$$|\vec{k}\rangle = \frac{1}{(2\pi)^{3/2}}e^{i\vec{k}\cdot\vec{r}} \tag{5.39}$$

we want to calculate

$$\vec{d}(\vec{k}) = \langle\vec{k}|\vec{r}|0\rangle = \frac{1}{2^{3/2}\pi^2}\int d^{(3)}r\, e^{-i\vec{k}\cdot\vec{r}}\vec{r}e^{-r} \tag{5.40}$$

We can obtain the dipole by an inner derivative with respect to $\vec{k}$:

$$\vec{d}(\vec{k}) = i\vec{\nabla}_k\langle\vec{k}|0\rangle = i\vec{\nabla}_k\left(\frac{1}{2^{3/2}\pi^2}\int d^{(3)}re^{-i\vec{k}\cdot\vec{r}}e^{-r}\right) \tag{5.41}$$

Using the expansion into spherical Bessel functions

$$e^{-i\vec{k}\cdot\vec{r}} = \sum_l (-i)^l (2l+1) j_l(kr) P_l(\cos\gamma), \tag{5.42}$$

where γ is the angle between $\vec{r}$ and $\vec{k}$: $rk\cos\gamma = \vec{k}\cdot\vec{r}$, and transforming to spherical coordinates we obtain

$$\langle\vec{k}|0\rangle = \frac{1}{2^{3/2}\pi^2}\int_0^{2\pi} d\varphi \int_{-1}^{1} d\cos\gamma \int_0^{\infty} dr r^2 \sum_l (-i)^l (2l+1) P_l(\cos\gamma) j_l(kr) e^{-r}. \tag{5.43}$$

The spherical symmetry of the initial state is reflected in the fact that all terms in the sum except $l = 0$ vanish upon integration over $\cos\gamma$, leading to

$$= \frac{2^{1/2}}{\pi}\int_0^{\infty} dr r^2 j_0(kr) e^{-r}. \tag{5.44}$$

Observing that $j_0(kr) = \sin(kr)/(kr)$ this integral can easily be evaluated leading to

$$\langle\vec{k}|0\rangle = \frac{\sqrt{8}}{\pi}\frac{1}{(1+k^2)^2} \tag{5.45}$$

and by differentiating with respect to $\vec{k}$ one obtains the dipole matrix element

$$i\vec{\nabla}_k\langle\vec{k}|0\rangle = i\frac{4\vec{k}}{1+k^2}\langle\vec{k}|0\rangle = \frac{i\sqrt{8}}{\pi}\frac{4\vec{k}}{(1+k^2)^3} \tag{5.46}$$

5.4 A crash course in variational calculus

A functional $F(\Psi)$ maps a function Φ belonging to some linear space of functions $\mathcal{H}$ (e.g. the Hilbert space) into the (complex) numbers. In that sense, the energy of quantum mechanics is a functional of the wave function Ψ:

$$E(\Psi) = \langle\Psi|H|\Psi\rangle. \tag{5.47}$$

Variational calculus is analogous to multi-dimensional calculus, but for "infinitely many" dimensions. Roughly speaking, if the gradient ∇ is a finite-length vector of derivatives, e.g. $\nabla = (\partial/\partial x_1, \partial/\partial x_2, \partial/\partial x_3, \partial/\partial x_4)$ in 4 dimensions, then the "functional derivative" produces the infinitely dimensional gradient of a functional.

The functional derivative is — in close analogy to the ordinary derivative —

$$\frac{\delta}{\delta\chi}F(\Psi) = \lim_{\epsilon\to 0}\frac{F(\Psi+\epsilon\chi) - F(\Psi)}{\epsilon}. \tag{5.48}$$

In general, the "variation" must be chosen such that $F(\Psi+\epsilon\chi)$ is defined. E.g. for the quantum mechanical energy, it must be possible to apply the Laplace operator $\Delta\chi$, i.e. χ should be twice differentiable.

Finite-dimensional calculus is a limiting case of the variational calculus: functionals on a n-dimensional space $\mathcal{H}$ can be simply written as functions of n variables $F(\Psi) = f(b_1, b_2, \ldots, b_n)$ for $\Psi = \sum_{i=1}^{n} b_i|i\rangle$ with some finite-dimensional basis $\{|i\rangle, i = 1, \ldots, n\}$. All functions $\chi = c_1|1\rangle + c_2|2\rangle, \ldots, c_n|n\rangle$. With that Eq. (5.48) turns into

$$\frac{\delta}{\delta\chi}F(\Psi) = \lim_{\epsilon\to 0}\frac{f(b_1+\epsilon c_1, b_2+\epsilon c_2, \ldots, b_n+\epsilon c_n) - f(b_1, b_2, \ldots, b_n)}{\epsilon} = \vec{c}\cdot\nabla f(b_1, b_2, \ldots, b_n). \tag{5.49}$$

A condition like

$$\frac{\delta}{\delta\chi}F(\Psi) = 0 \quad \forall\chi \in \mathcal{H} \tag{5.50}$$

in finite dimensions corresponds to

$$\vec{c}\cdot\nabla f = 0 \quad \forall\vec{c}. \tag{5.51}$$

One often uses the notation "$\delta F(\Psi)$" for $\frac{\delta}{\delta\chi}F(\Psi) = 0 \quad \forall\chi$ and uses the notation $\chi := \delta\Psi$.

These are all formal considerations, the important mathematical questions have to do with existence of the limits and the possible choices for χ, but this does not concern us here.

5.4.1 Variations of the energy functional

Eigenenergies are associated with stationary points of the energy functional, i.e.

$$0 = \epsilon\delta\langle\Psi|H|\Psi\rangle = \langle\Psi+\epsilon\delta\Psi|H|\Psi+\epsilon\delta\Psi\rangle - \langle\Psi|H|\Psi\rangle = \langle\epsilon\delta\Psi|H|\Psi\rangle - \langle\Psi|H|\epsilon\delta\Psi\rangle, \tag{5.52}$$

where we have dropped the term of order ϵ^2. Dividing by ϵ, we find the condition

$$0 = \langle\delta\Psi|H|\Psi\rangle + \langle\Psi|H|\delta\Psi\rangle \quad \forall\delta\Psi. \tag{5.53}$$

For selfadjoint ($\approx$ hermitian) H, condition (5.53) is equivalent to

$$0 = \langle\delta\Psi|H|\Psi\rangle \quad \forall\delta\Psi. \tag{5.54}$$

This can be seen as follows:

$$0 = \langle\delta\Psi|H|\Psi\rangle + \langle\Psi|H|\delta\Psi\rangle = \langle\delta\Psi|H|\Psi\rangle + \langle\delta\Psi|H|\Psi\rangle^* = 2Re\langle\delta\Psi|H|\Psi\rangle \quad \forall\Psi. \tag{5.55}$$

Assume Ψ fulfills (5.55), but there exists a $\delta\Psi_1$ such that $Im\langle\delta\Psi_1|H|\Psi\rangle \neq 0$. Then we can choose $\delta\Psi_0 = i\delta\Psi_1$ and we obtain

$$Re\langle\delta\Psi_0|H|\Psi\rangle = Re\langle i\delta\Psi_1|H|\Psi\rangle = Re(-i)\langle\delta\Psi_1|H|\Psi\rangle = Im\langle\delta\Psi_1|H|\Psi\rangle \neq 0. \tag{5.56}$$

which contradicts (5.55).

5.4.2 TDSE: Dirac-Frenkel variational principle

In this approach, the action functional should have a stationary point

$$\delta \int_{t_0}^{t_1} \langle \Psi(t) | [id/dt - H(t)]\Psi(t)\rangle / \langle \Psi(t)|\Psi(t)\rangle dt = 0. \tag{5.57}$$

The explicit normalization of the wave function is needed to remove surface terms when one moves d/dt to the left side by partial integration. A similar analysis as above leads to

$$0 = \langle \delta\Psi | Q(id/dt - H)\Psi\rangle + \langle Q(id/dt - H)\Psi | \delta\Psi\rangle = 2Re\langle \delta\Psi | Q(id/dt - H)\Psi\rangle \tag{5.58}$$

where $Q = 1 - |\Psi\rangle(\langle\Psi|\Psi\rangle)^{-1}\langle\Psi|$ projects onto the space orthogonal to $|\Psi\rangle$. Using the same reasoning as above, this is equivalent to

$$\langle \delta\Psi | Qid/dt - H(t)|\Psi\rangle = 0. \tag{5.59}$$

$$\langle \delta\Psi | id/dt - H(t)|\Psi\rangle = 0. \tag{5.60}$$

In practice, presentation of $|\Psi\rangle$ in some fixed basis, say,

$$|\Psi\rangle = \sum_{i=1}^{\infty} b_i |i\rangle \tag{5.61}$$

we can represent all possible variations in the form

$$|\delta\Psi\rangle = \sum_{i=1}^{\infty} \delta b_i |i\rangle. \tag{5.62}$$

The Dirac-Frenkel variational principle then reads

$$\sum_i \delta b_i^* \langle i | id/dt - H(t)|\Psi\rangle = 0. \tag{5.63}$$

The meaning of the Dirac-Frenkel principle is as follows: assume you try to solve the TDSE in some space spanned by the basis $\{|i\rangle\}$, which may be the space where the exact solution is located, or some reduced space, say, a finite-dimensional approximation to the Hilbert space. Let $|e\rangle$ be a possible error in fulfilling the equation

$$|e\rangle = [id/dt - H(t)](|i\rangle b_i) \tag{5.64}$$

then the Dirac-Frenkel principle says, that this error should be *outside* the space of our possible solutions

$$\langle \delta\Psi | e\rangle = 0 \quad \forall \delta\Psi \in \mathcal{H}. \tag{5.65}$$

5.4.3 Constraints on the allowed variations

If, as in our case of the SFA ansatz, the b_i are subjected to some constraint of the general form $f(\vec{b}) = 0$, a variation under that constraint can be implemented by the method of Lagrange multipliers, which means that

$$\sum_k \delta b_k^* \langle k|id/dt - H(t)|\Psi\rangle + \lambda \delta f(\vec{b}) = 0, \tag{5.66}$$

for some Lagrange multiplier λ which is determined by substituting into the constraint.

5.4.4 Alternative derivation of the SFA

Time-dependent perturbation theory

Time-dependent perturbation theory relies on the simple mathematical identity

Dyson equation

$$U(t,t_0)\Psi(t_0) = U_0(t,t_0)\Psi(t_0) + i\int_{t_0}^{t} dt' U(t,t')V(t')U_0(t',t_0)\Psi(t_0) \tag{5.67}$$

with the (atomic) ground state as initial state $\Psi(t_0)$ with

$$\frac{d}{dt'}U_0(t,t') = iU_0(t,t')H_0 \qquad \frac{d}{dt'}U(t',t_0) = -i[H_0 + V(t)]U(t',t_0) \tag{5.68}$$

Note that $V(t)$, in general, does not commute with $U_0(t,t')$. For our problem, set Set $H_0 = -\Delta/2 - 1/r$ and $V(t) = -\vec{\mathcal{E}}(t)\cdot\vec{r}$.

The strong field approximation results by replacing the full propagator under the integral with the free propagator in the field (Volkov propagator)

$$U(t,t') \;\rightarrow\; U_V(t,t') = \int d^3k\, |\vec{k},t\rangle\langle\vec{k},t'| \tag{5.69}$$

$$= \int d^3k\, e^{i[\vec{k}-\vec{A}(t)]\cdot\vec{r}} e^{-i\int_{t'}^{t}\frac{1}{2}\left[\vec{k}-\vec{A}(\tau)\right]^2 d\tau} \int d^{(3)}r'\, e^{-i[\vec{k}-\vec{A}(t)]\cdot\vec{r}'}(\cdot) \tag{5.70}$$

which leads directly to the SFA.

5.4.5 A comment on gauges

The Dyson-type derivation is much more compact, but does not expose as clearly the main physical idea of SFA: *assume* the main part of the wave remains in the field free ground state. Anything that is not in the ground state, is in a free (Volkov) state, which is more clearly exposed in the first, more complicated derivation.

The Dyson-type derivation of the SFA may be responsible for much of the confusion concerning which gauge is the right gauge to use: we may write the Volkov propagator

in either gauge. However, by doing so, we change our physical picture. In velocity gauge, we do *not* assume that the system remains mostly in the field free ground state. Rather, the also the bound electron experiences a time dependent boost (change of momentum). However, this possibly quite violently shaken bound electron is quite unphysical. In "reality", it just would not remain bound...

Chapter 6

High harmonic generation

Idea: an electron is detached and accelerated by the field and recombines with the atom; the resulting photon energy may be higher than the original one.

6.1 The classical model

recollision condition

$$0 = z(t_0) - z(t_1) = \int_{t_0}^{t_1} v(t)dt = -\int_{t_0}^{t_1} dt \int_{t_0}^{t} \mathcal{E}(t')dt'. \tag{6.1}$$

With the condition that $\dot{z}(t_0) = 0$ we get:

$$A(t_0)(t_1 - t_0) = \int_{t_0}^{t_1} dt A(t). \tag{6.2}$$

This is the *recollision condition.*

Recollision energy

$$\frac{\dot{z}^2}{2} = \frac{[A(t_1) - A(t_0)]^2}{2}. \tag{6.3}$$

The maximal difference is $2A_0$, but that cannot be reached, as it would require release at maximum positive A and recollision at maximal negative A. For such points the recollision condition cannot be met.

Numerically determine t_0 and t_1:

$$\omega t_0 \approx -0.45 \times 2\pi, \tag{6.4}$$

$$\omega t_1 \approx 0.2 \times 2\pi. \tag{6.5}$$

For these times, the recollision energy is

$$\frac{1}{2}|\cos(-0.9\pi) - \cos(0.4\pi)|^2 A_0^2 = 1.585\frac{A_0^2}{2} = 3.17U_p. \tag{6.6}$$

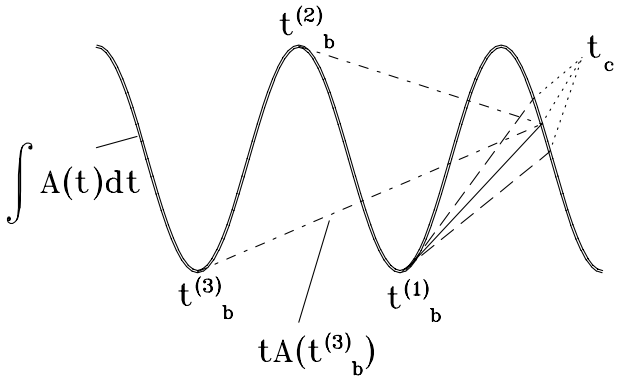

Figure 6.1: recollision condition, graphical solution of Eq. (6.2). The straight lines connecting release times $t_i^{(i)}$ with recollision time t_c have slopes $A(t_i)$. recollisions occur, where the straight lines intersect with the integral over $A(t)$. A given t_c is reached from several different $t_i^{(i)}$ (dot-dashed and solid lines). The birth time $t_i^{(1)}$ leads to maximum recollision energy. Electrons released slightly before and after $t_i^{(1)}$ re-collide later and earlier, respectively, with lower recollision energies ("long" and "short" trajectories, dashed lines).

Harmonic cutoff frequency ω_{cutoff}

The maximal photon energy that can be released at recollision is the sum of kinetic recollision energy and the binding energy of the atom

$$\omega_{\text{cutoff}} = |E_0| + 3.17U_p.$$

Why only *harmonics*, i.e. multiples of the fundamental frequency? — arise in *long* pulses, i.e. where the recollision process is periodically repeated at period $2\pi/\omega$ (even and odd harmonics), or, if positive and negative half-cycles have generate the same process, at period π/ω (only odd harmonics).

Long and short trajectories

All energies, except for the maximal energy, are produced twice during a single half-cycles, see Fig. 6.1. At the same energy, later release times lead to earlier recollision $\Rightarrow$*short trajectory*, earlier release times $\Rightarrow$*long trajectory*. This matters for phase-matching (see also Figure 7.1).

6.2 A quantum calculation

We need to know the response of an atom to the field. Dipole part of the polarization of an atom = probability distribution of the electron $\times$ distance of the electron from the

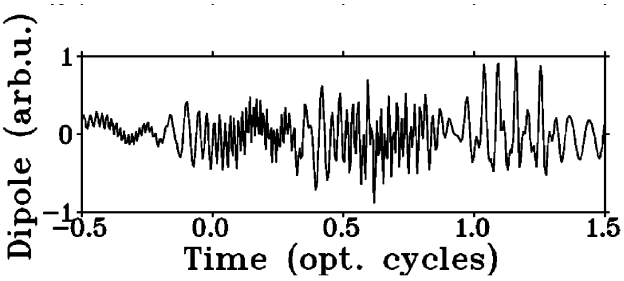

Figure 6.2: (Numerical simulation) The dipole response $P(t)$ of an atom to a strong few-cycle pulse. No clear structures are discernable. System parameters: hydrogen atom, laser pulse intensity $4 \times 10^{14} W/cm^2$, duration 5 fs FWHM, wave length 800 nm.

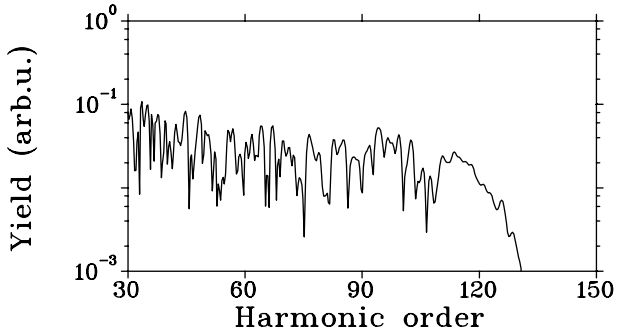

Figure 6.3: (Numerical simulation) Harmonic spectrum $h(\omega)$ derived from the dipole response in figure 6.2 by Eq. (6.8). Plateau and cutoff can be well distinguished. The cutoff is smooth, but in the plateau no regularities can be discerned.

nucleus:

$$\vec{P}_d(t) = \int d\vec{r} |\Psi(\vec{r},t)|^2 \vec{r} = \langle \Psi(t) | \vec{r} | \Psi(t) \rangle \tag{6.7}$$

Harmonic spectrum

The *acceleration* of the polarization is the source of new radiation $\propto \ddot{P}(t)$, the "harmonic" radiation (if multiples of the fundamental).

Obtain $\Psi(t)$ by numerically solving the TDSE. The harmonic response is proportional to the Fourier transform

$$\vec{h}(\omega) = (2\pi)^{-1/2} \int dt e^{i\omega t} \ddot{\vec{P}}(t) = -(2\pi)^{-1/2} \omega^2 \int dt e^{i\omega t} \vec{P}(t) \tag{6.8}$$

Time-frequency analysis of $\ddot{P}(t)$

Slide a window function over the signal and Fourier transform. For a time-frequence power spectrum, take the modulus squared:

$$H(\omega, t) = |\mathcal{F}[\ddot{P}(t') e^{-(t-t')^2/T^2}]| \tag{6.9}$$

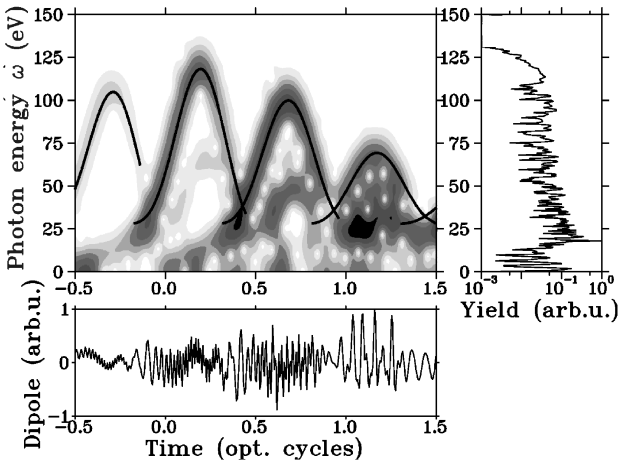

Figure 6.4: Time-frequency analysis of the the dipole response Fig. 6.2. The lower panel shows the numerically calculated dipole response. The time-frequency analysis of the signal obtained by Fourier-transforming with a Gaussian window function is given in the upper panel. Solid lines indicate the recombination energies obtained by the classical model. Photons with energies $\sim 120\,eV$ are only emitted during a few hundred attoseconds after $t = 0$. The total harmonic spectrum is shown to the right.

For desired resolution starting from ∼20th harmonic a good choice for the window function $T = 0.05 \times 2\pi/\omega_{\text{laser}}$

$\Rightarrow$ resolve only harmonics $N\omega_{\text{laser}}$, $N \lesssim 20$

Looking at figure 6.4 we conclude

The recollision model captures all essential physical processes of HHG

6.3 The Lewenstein model

[Lewenstein et al., PRA **49**, 2117 (1994)]

$\Psi(\vec{r}, t)$ in Strong Field Approximation (SFA):

$$|\Psi\rangle = |0\rangle + \int d\vec{k} b(\vec{k}, t)|\vec{k}, t\rangle, \tag{6.10}$$

and the dipole moment

$$\langle\Psi|\vec{r}|\Psi\rangle = \underbrace{\langle 0|\vec{r}|0\rangle}_{=0:\,\text{symmetry}} + \int d\vec{k}\langle 0|\vec{r}|\vec{k}\rangle b(\vec{k}, t) + h.c. + \underbrace{\int d\vec{k} \int d\vec{k}' b^* b \langle\vec{k}'|\vec{r}|\vec{k}\rangle}_{\text{neglect}}, \tag{6.11}$$

$$\vec{P}(t) \approx +2\mathcal{R}e \int d\vec{k}\langle 0|\vec{r}|\vec{k}\rangle b(\vec{k}, t).$$

More explicitly (restrict field to z-direction $\Rightarrow$ ($\vec{P}$) is in z-direction only.

$$P_z = 2\mathcal{R}e \int d\vec{k} \int_{-\infty}^{t} dt' \underbrace{e^{iE_0 t} d_z^*[\vec{k} - \vec{A}(t)]}_{\text{(3) recombination}} \underbrace{e^{\frac{i}{2}\int_{t'}^{t}[\vec{k}-\vec{A}(\tau)]^2 d\tau}}_{\text{(2) free propagation}} \underbrace{e^{-iE_0 t'} \mathcal{E}_z(t') d_z[\vec{k} - \vec{A}(t')]}_{\text{(1) ionization}}. \quad (6.12)$$

3-step model: (tunnel-)ionization, propagation, recombination

Integrals by the stationary phase method

(2) is a rapidly oscillating phase. $\Rightarrow$ the dominant contributions come from the range of minimal change of the phase

"stationary phase"

Math: the stationary phase method

Assume you have an integral of the general form

$$I[g, \phi] = \int_{-\infty}^{\infty} dt g(t) e^{i\phi(t)}. \quad (6.13)$$

In the case $\phi(t) = \omega t$ we obtain just the value of the Fourier transform at the frequency ω. Now let us assume that we have something like the usual separation like in a laser pulse into an "envelope" $g(t)$ and a "carrier" $e^{\omega t}$, where the envelope is assumed to be slowly varying compared to the oscillations of the carrier (cf. Fig. 6.5(a)). Let us further assume that the oscillation period is not constant, but varies in time, and that there is a time t_s where it even reaches zero, i.e. $\phi'(t) = 0|_{t=t_s}$ (cf. Fig. 6.5(b)). The most important contribution to the integral comes from area around the stationary point t_s. Let us expand the phase around the stationary point t_s in the form

$$\phi(t) = \phi(t_s) + \underbrace{\phi'(t_s)}_{=0}(t - t_s) + \frac{\phi''(t_s)}{2}(t - t_s)^2 + O(t - t_s)^3 \quad (6.14)$$

Keeping only the terms quadratic in t_s and neglecting the t-dependence of the envelope $g(t)$ in the region around t_s we obtain the approximate integral

$$I[g, \phi] \approx= g(t_s) e^{i\phi(t_s)} \int_{-\infty}^{\infty} e^{\frac{\phi''(t_s)}{2}(t-t_s)^2} dt, \quad (6.15)$$

which leads to

$$I[g, \phi] \approx= \sqrt{\frac{\pi}{|t - t_s|}} e^{i\pi/4} g(t_s) e^{i\phi(t_s)} \quad (6.16)$$

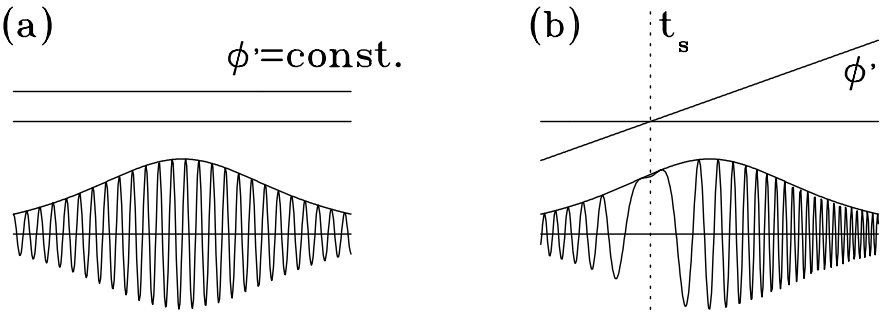

Figure 6.5: Stationary phase integration.

6.3.1 Stationary phase integration over $\vec{k}$

$$\vec{\nabla}_k \int_{t'}^{t} [\vec{k} - \vec{A}(\tau)]^2 d\tau \stackrel{!}{=} 0 = 2\int_{t'}^{t} \vec{k} - \vec{A}(\tau) d\tau. \tag{6.17}$$

For given t, t' the dominant contribution to the integral comes from momentum

$$\vec{k}(t,t') := \frac{1}{t-t'}\int_{t'}^{t} \vec{A}(\tau)d\tau \simeq \overline{\vec{A}(\tau)}|_{\tau\in[t,t']} \quad . \tag{6.18}$$

This is just the condition that an electron, which is released at time t' from position 0 with a canonical momentum $\vec{k}$, returns to that position at time t. For that we remember that the canonical momentum $\vec{k}$ is constant in velocity gauge, and that the physical momentum is given by

$$\vec{v}(\tau) = [\vec{k} - \vec{A}(\tau)]/m. \tag{6.19}$$

The condition $\int_{t'}^{t} \vec{v}(\tau)d\tau$ is equivalent to Eq. (6.18). In particular, with the initial condition $\vec{v}(t') = 0$ we have $\vec{k} = \vec{A}(t')$ and we recover our classical recollision condition $\int \vec{A}(\tau)d\tau = \vec{A}(t')(t'-t) = 0$ (c.f. Fig. 6.1). However, we have not yet derived this initial condition from our SFA Schrödinger equation.

Integrate near $k(t,t')$

$$\vec{k} = \vec{k}(t,t') + \vec{q} \tag{6.20}$$

$$\int d\tau[\vec{k} - \vec{A}(\tau)]^2 = \int d\tau[\vec{k}(t,t') - \vec{A}(\tau)]^2 + 2\vec{q}\underbrace{\int d\tau[\vec{k}(t,t') - \vec{A}(\tau)]}_{=0} + (t-t')\vec{q}^2 \tag{6.21}$$

$$\begin{aligned}
& \int d\vec{k} d_z^*[k - A(t)]e^{-\frac{i}{2}\int_{t'}^{t}[k+\vec{A}(\tau)]^2 d\tau} e^{-iE_0 t'} d_z[\vec{k} - \vec{A}(t')] \\
\approx & \int d\vec{q} d_z^*[\vec{k} - \vec{A}(t)]e^{-\frac{i}{2}\int_{t'}^{t}[\vec{k}(t,t')+\vec{q}-\vec{A}(\tau)]^2 d\tau} e^{-iE_0 t'} d_z[\vec{k} - \vec{A}(t')] \\
= & \; d_z^*[\vec{k} - \vec{A}(t)]e^{-\frac{i}{2}\int_{t'}^{t}[\vec{k}(t,t')-\vec{A}(\tau)]^2 d\tau} e^{-iE_0 t'} d_z[\vec{k} - \vec{A}(t')] \int d\vec{q} e^{-\frac{i}{2}(t-t')\vec{q}^2}
\end{aligned}$$

For this derivation, at one point we have neglected the $\vec{q}$ dependence of the dipole matrix elements

$$d_z[k - A(t)] = d_z[k(t,t') + q - A(t)] \approx d_z[k(t,t') - A(t)]. \tag{6.22}$$

This implies that the element varies slowly in the surrounding of the recollision momentum $k(t,t')$.

Performing the remaining integral over $\vec{q}$, we obtain

A "diffusion" term

$$\int d\vec{q} e^{-\frac{i}{2}(t-t')\vec{q}^2} = \left(\frac{2\pi}{t-t'}\right)^{3/2} \tag{6.23}$$

Using (6.23) we finally complete the saddle point integration over $\vec{k}$:

$$= \int dt' \left(\frac{2\pi}{t-t'}\right)^{3/2} e^{-i\int_{t'}^{t} \frac{1}{2}[\vec{k}(t,t')-A(\tau)]^2 d\tau - iE_0(t-t')} \mathcal{E}(t) d_z^*[\vec{k} - \vec{A}(t)] d_z[\vec{k} - \vec{A}(t')] \tag{6.24}$$

Up to an attenuation by diffusion only the classical paths contribute to the integrals

6.3.2 Integration over t'

Again we can assume that the main contribution to the integral comes from the point where the phase changes the least. The stationary phase condition with respect to t' reads

$$\frac{\partial}{\partial t'} \int_{t'}^{t} -\frac{i}{2}[\vec{k}(t,t') - A(\tau)]^2 d\tau - iE_0(t-t') = 0 \tag{6.25}$$

or

$$\frac{1}{2}[\vec{k}(t,t') - A(t')]^2 = E_0 \tag{6.26}$$

Note that this condition can never be fulfilled for real t' as $E_0 < 0$. However, it can be fulfilled if we analytically continue our integrand into the complex plane of t. This is possible, if $A(\tau)$ and d are "sufficiently" analytic.

Problem

Using the explicit form of the hydrogen dipole transition matrix element Eq. (5.46) with the hydrogen ground state energy $2E_0 = -1$ we find

$$d(k - A) \propto \frac{\vec{k} - \vec{A}}{[-2E_0 + (\vec{k} - \vec{A})^2]^3}. \tag{6.27}$$

Our dipole matrix elements are *singular* at the stationary phase point! The function in our integrand does not have the form of (smooth)×(rapidly oscillation), but rather

(singular)×(rapidly oscillation). Still it is fair to assume that the dominant contribution comes from that point, but one must be careful when evaluating the integral.

The singularity is not a coincidence: it is connected to the fact that there is a bound state in the field free case exactly at the (negative) energy that also shows up in the exponent. It will therefore be there in any case.

One can, in principle, work around those problems by performing the integrals over the function 'exponential × singularity' and obtain a solution. However, let us look at the meaning of the integral over t': it is the same type of integral as (5.36), the amplitude of ionization. As mentioned there, there is a serious approximation in this amplitude by neglecting $V_\perp$, which gives incorrect ionization yields.

A factorization

In [M.Yu. Ivanov, PRA **54**, 742 (1996)] the following form of the integral is derived (using saddle point integration)

$$P(t) = \sum_{t_b} \frac{1}{\sqrt{i}} a_{ion}(t_b) a_{pr}(t_b, t) a_{rec}(t) + h.c. \tag{6.28}$$

t_b "birth time", i.e. the moment when the electron is detached. If we want to recollide an electron at time t, we get the corresponding birth time as solution of the recollision condition (6.2):

$$A(t_b) = \frac{1}{t - t_b} \int_{t_b}^{t} dt' A(t') =: k(t, t_b). \tag{6.29}$$

This equation may have several solutions, hence the sum in (6.28).

a_{ion} (square root) of the static field ionization rate at time t_b

$$= \sqrt{\frac{dn(t)}{dt}} \tag{6.30}$$

for small depletion $\approx \sqrt{\Gamma(\mathcal{E}(t))}$

a_{pr} the free propagation along classical trajectories (E_0 = ground state energy)

$$= \left(\frac{2\pi}{t - t_b}\right)^{3/2} \frac{(-2E_0)^{1/4}}{\mathcal{E}(t_b)} \exp\left[-\frac{i}{2}\left(\int_{t_b}^{t} dt' [k(t, t_b) - A(t')]^2\right) + iE_0(t - t_b)\right] \tag{6.31}$$

a_{rec} dipole transition to the ground state at t

$$= d^*[\vec{k}(t, t_b) - \vec{A}(t)] \tag{6.32}$$

NOTE: From the saddle point analysis, one obtains dn/dt **in strong field approximation**. Due to the approximation $V_\perp = 0$, this rate is incorrect. An obvious correction of the formula above is to use the *exact* (e.g. ADK or numerical) $\Gamma(\mathcal{E}(t))$.

6.3.3 Harmonic spectrum

[V.S. Yakovlev, PhD thesis]

a_{ion} and a_{rec} both are slowly varying functions of t. *Rapid oscillations* come from the phase

$$\exp\left[-i\frac{1}{2}\int_{t_b}^{t} dt'[k(t,t_b)-A(t')]^2 + iE_0(t-t_b)\right] \approx \exp\left[-i\omega(t_b,t)t\right], \tag{6.33}$$

where

$$\begin{aligned}
\omega(t_b,t) &= \frac{d}{dt}\left[\frac{1}{2}\int_{t_b}^{t} dt'[k(t,t_b)-A(t')]^2 - E_0(t-t_b)\right] \\
&= \frac{1}{2}\left[k(t,t_b)-A(t)\right]^2 - E_0 - \frac{1}{2}\underbrace{\left[k(t,t_b)-A(t_b)\right]^2}_{=0:\,\vec{v}(t_b)=0}\frac{dt_b(t)}{dt} && (6.34)\\
&\quad + \underbrace{\frac{1}{2}\int_{t_b}^{t} dt'\frac{d}{dt}[k(t,t_b)-A(t')]^2}_{=0\ \text{stat phase}\ k(t,t_b)} && (6.35)\\
&\quad - \frac{1}{2}\underbrace{\int_{t_b}^{t}\frac{d}{dt_b}[k(t,t_b)-A(t')]^2}_{=0:\,\text{stat phase}\,k(t,t_b)}\frac{dt_b(t)}{dt} + E_0\frac{dt_b(t)}{dt} && (6.36)\\
&= \frac{1}{2}[k(t,t_b)-A(t)]^2 - E_0 + \frac{dt_b}{dt}E_0. && (6.37)
\end{aligned}$$

NOTE

(1) $\partial_t k(t,t_b)$ does not contribute (because of the stationary phase condition)

(2) we also use $k(t,t_b)-A(t_b)=0$, i.e. initial velocity = 0

$t_b(t)$:

$$A(t_b)(t-t_b) = \int_{t_b}^{t} A(\tau)d\tau. \tag{6.38}$$

$\partial/\partial t$:

$$\frac{\partial A}{\partial t_b}\frac{\partial t_b}{\partial t}(t-t_b) + A(t_b)(1-\frac{\partial t_b}{\partial t}) = A(t) - \frac{\partial t_b}{\partial t} + A(t_b), \tag{6.39}$$

from which we obtain

$$\frac{\partial t_b}{\partial t} = -\frac{A(t)-A(t_b)}{\mathcal{E}(t_b)(t-t_b)}, \tag{6.40}$$

$$\omega(t_b,t) = \frac{1}{2}[\underbrace{k(t,t_b)}_{\approx A(t_b)} + A(t)]^2 - E_0[1+\underbrace{\frac{A(t)-A(t_b)}{\mathcal{E}(t_b)(t-t_b)}}_{\approx 0.4}]. \tag{6.41}$$

The approximate value of 0.4 for the last term is a numerical finding that holds in the typical range of $\lambda = 800\,nm$ and for harmonic energies near and below 100 eV. Under different conditions it needs to be re-calculated.

Harmonic energies as a function of time

$$\omega(t_b, t) = \frac{[A(t_b) - A(t)]^2}{2} - 1.4E_0. \qquad (6.42)$$

Size of the quantum correction to t_b

In the derivation above, we use our *classical* reasoning $\vec{v}(t_b^{(cl)}) = 0 = k(t_b^{(cl)}, t) - A(t_b)$, from which we obtain a classical birth time . The correction shows, to which extend this fails: if instead we were to use the saddle point birth time with the condition

$$\frac{1}{2}[k(t_b^{(sd)}, t) - A(t_b^{(sd)})]^2 - E_0 = 0, \qquad (6.43)$$

no correction term would appear, but $t_b^{(sd)} \neq t_b^{(cl)}$.

Chapter 7

Pulse propagation

7.0.4 Phase matching of long and short trajectories

The Gaussian beam

$$\mathcal{E}(r,z) = \mathcal{E}_0 \frac{w_0}{w(z)} \exp\left(\frac{-r^2}{w^2(z)}\right) \exp\left(-ikz - ik\frac{r^2}{2R(z)} + i\zeta(z)\right). \tag{7.1}$$

Here we have use the beam waist

$$w(z) = w_0 \sqrt{1 + \left(\frac{z}{z_0}\right)^2} \tag{7.2}$$

and the Rayleigh range (of depth of focus)

$$z_0 = \frac{\pi w_0^2}{\lambda} \tag{7.3}$$

Accross the focus, the phase of the driver pulse changes by the purely geometrical Guoy-phase

$$\zeta(z) = \arctan\left(\frac{z}{z_0}\right) \tag{7.4}$$

with an overall phase change of π. This phase change corresponds to a flipover of the electrical field and has its correspondence in wave-optics as the crossing of two optical rays in the focus, where up and down is interchanged.

In turn, the phase of harmonic generation is determined by the time (more precise the action integral accumulated) between electron emission an recollision. These times vary with intensity: for fixed frequency, the short trajectories become shorter with increasing pulse intensity, while the long trajectories become longer (cf. Fig. 7.1).

7.0.5 First order propagation equation

The following wave-equation is a direct consequence of Maxwell's equations in a polarizable medium:

$$\left[\partial_z^2 + \Delta_\perp - \frac{1}{c^2}\partial_t^2\right] \mathcal{E}(\vec{r},t) = \frac{1}{\epsilon_0 c^2}\partial_t^2 \left[P_L(\vec{r},t) + P_{NL}(\vec{r},t)\right]. \tag{7.5}$$

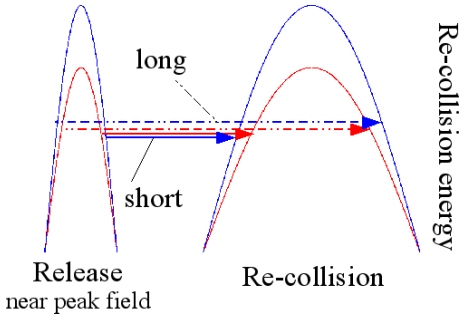

Figure 7.1: Variation of the long and short trajectories with laser intensity at a given re-collision energy (vertical displacement of the arrows). Withincreasing intensity, long trajectories start earlier and recollied later. For short trajectories it is the reverse

We denote the most general linear part of the polarization response as

$$P_L(\vec{r},t) = \int_{-\infty}^{t} \chi^{(1)}(t')\mathcal{E}(t-t')dt' \tag{7.6}$$

and separate it from the rest, the non-linear polarization P_{NL}. Here $\Delta_\perp = \partial_x^2 + \partial_y^2$ As a simplifying assumption we assumed that the response does not change polariation and we have dropped the vector signs over $\vec{\mathcal{E}}$ and $\vec{P}$. Fourier transform with respect to time leads to the full (2nd order) propagation equation in frequency space:

$$\left[\partial_z^2 + \Delta_\perp + k^2(\omega)\right]\mathcal{E}(\vec{r},\omega) = \frac{\omega^2}{\epsilon_0 c^2}\mathcal{F}\left[P_{NL}(\vec{r},t)\right] \tag{7.7}$$

For notational simplicity, we distingush $\mathcal{E}(\vec{r},t)$ and its Fourier transform only $\mathcal{E}(\vec{r},\omega)$ only the different arguments t and ω. By $k(\omega)$ we denote the linear dispersion.

Note: scalar equations for $\mathcal{E}$; i.e. we assume no change of polarization. This is OK for a gently focussed beam in a (nearly) isotropic medium as a gas jet

Defining $\mathcal{E} = e^{-ik\cdot z}\tilde{U}$ and inserting this in the above propagation equation, we obtain the following equation for the envelope $\tilde{U}$:

$$\left[\partial_z^2 + 2ik\partial_z + \Delta_\perp\right]\tilde{U} = \frac{\omega^2}{\epsilon_0 c^2}\exp[-ik(\omega)z]\mathcal{F}\left[P_{NL}(\vec{r},t)\right] \tag{7.8}$$

7.0.6 Slowly evolving wave approximation

Neglect $\partial_z^2\tilde{U}$: admissible when the pulse changes little during propagation over one wave length.
This condition can be reformulated as follows:
Change coordinates to a *moving frame of reference*

$$(t,z) \longrightarrow (\tau,\xi) = (t - z/v_0, z) \tag{7.9}$$

$$\partial_\xi \mathcal{E} \ll k\mathcal{E} \tag{7.10}$$

Back to the field $\mathcal{E}(\omega)$:

$$\left[\partial_z - ik(\omega) - \frac{i}{2k(\omega)}\Delta_\perp\right]\mathcal{E}(\omega) = -i\frac{\omega}{2\epsilon_0 n(\omega)c}\mathcal{F}[P_{NL}] \tag{7.11}$$
$$n(\omega) = k(\omega) \times (c/\omega)$$

7.0.7 Non-linear polarization P_{NL}

High frequency response $\Longrightarrow$ high harmonic generation

Low frequency response: dominated by ionization and free electrons

Total free electrons

$$n_e(t) = n_{atoms}\left(1 - \exp\left[-\int_{-\infty}^{t}\Gamma(\mathcal{E}(t'))dt'\right]\right) \tag{7.12}$$

Polarization

$$\vec{P}_{NL}(t,\vec{r}) = n_e(t,\vec{r})\vec{r} \tag{7.13}$$

Time-derivative

$$\frac{d}{dt}\vec{P}_{NL} = n_e(t,\vec{r})\dot{\vec{r}} + \partial_t n_e(t,\vec{r})\vec{r} \approx n_e(t,\vec{r})\dot{\vec{r}} + \partial_t n_e(t,\vec{r})z_0\vec{e}_z \tag{7.14}$$

(Classical) point of electron release $\vec{r}_0$:

$$z_0 = -\frac{E_0}{\mathcal{E}(t)}, \qquad x_0 = y_0 = 0.$$

First term is the usual free electron response, second term is the change of electron density due to ionization; the second term becomes important, when there is significant ionization during a single laser cycle.

Note: It is assumed the the change of the electron denstity is strongly dominated by the release of electrons at the point $(0, 0, z_0)$.

Second derivative:

$$\frac{d^2}{dt^2}\vec{P}_{NL} = n_e(t,\vec{r})\ddot{\vec{r}} + \partial_t n_e(t,\vec{r})\dot{\vec{r}} - E_0\frac{d}{dt}[\frac{\partial_t n_e(t,\vec{r})}{\mathcal{E}(t)}]\vec{e}_z \tag{7.15}$$

Note: $\partial_t n$ is $\neq 0$ only at the point of electron release, but at that point $\dot{\vec{r}} \approx 0 \Rightarrow \partial_t n_e(t,\vec{r})\dot{\vec{r}} \approx 0$, since the initial velocity of a released electron is ≈ 0.

Back to first derivative ($\ddot{\vec{r}} = -\mathcal{E}$):

$$d/dtP_{NL} = -\int^t dt' n_e(t', \vec{r})\mathcal{E}(t') - E_0 \frac{\partial_t n_e(t, \vec{r})}{\mathcal{E}(t)} \tag{7.16}$$

Approximation:

$$n(\omega) \approx 1, \qquad k(\omega) \approx \omega/c \tag{7.17}$$

$$\left[\partial_z - i\frac{\omega}{c} - \frac{ic}{2\omega}\Delta_\perp\right]\mathcal{E}(\omega) = i\frac{1}{2\epsilon_0 c}\mathcal{F}[d/dtP_{NL}] \tag{7.18}$$

Back-fourier transform:

$$\left[\partial_z + \frac{1}{c}\partial_t\right]\mathcal{E} = \frac{c}{2}\nabla_\perp^2 \int_{-\infty}^t dt'\mathcal{E} - \frac{e^2}{2\epsilon_0 c}\int_{-\infty}^t dt' n_e \mathcal{E} - \frac{E_0}{2\epsilon_0 c}\frac{\partial_t n_e}{\mathcal{E}} \tag{7.19}$$

$$\begin{aligned} \frac{i}{\omega} &\rightarrow \int_{-\infty}^t dt' \\ -i\omega &\rightarrow \partial_t \end{aligned}$$

7.0.8 Separation of fundamental and harmonic field

When the harmonic intensity remains a small fraction of the original laser intensity, the propagation equation can be separated into two parts, one describing the propagation of the laser pulse with the strongly non–linear response of the medium and a second one, where the non–linear laser pulse acts as a source of harmonic radiation, which by itself does not interact non–linearly with the medium. The total electric field is split as follows

$$\mathcal{E} = \mathcal{E}_l + \mathcal{E}_h \tag{7.20}$$

What results are the two coupled equations

$$\begin{aligned} \partial_\xi \mathcal{E}_l(\xi,\tau) &= (c/2)\nabla_\perp^2 \int_{-\infty}^t d\tau' \mathcal{E}_l(\xi,\tau') - \frac{e^2}{2\epsilon_0 c}\int_{-\infty}^\tau n_e \mathcal{E}_l(\xi,\tau')d\tau' \\ &\quad -\frac{E_0}{2\epsilon_0 c}\frac{\partial_\tau n_e(\xi,\tau)}{\mathcal{E}_l(\xi,\tau)} - \frac{\zeta^{(1)}}{c}\partial_\tau\left(1 - n_e(\xi,\tau)\right)\mathcal{E}_l(\xi,\tau), \end{aligned} \tag{7.21}$$

where the nonlinear polarization is written in the simple form derived above and for the harmonic electric field $\mathcal{E}_h$,

$$\left(\partial_\xi + \alpha_h\right)\mathcal{E}_h(\xi,\tau) - (c/2)\nabla_\perp^2 \int_{-\infty}^t d\tau' \mathcal{E}_h(\xi,\tau') = \frac{-1}{2\epsilon_0 c}\partial_\tau P_h[\mathcal{E}_l(\xi,\tau)] + c.c.. \tag{7.22}$$

For computational convenience we have written the equations in a moving frame of reference $(z,t) \rightarrow (\xi = z, \tau = t - z/c)$. Absorption of the harmonics by the medium is described by the absorption coefficient α_h. The term containing $\zeta^{(1)}$ is a linear response term of the neutral atoms that was neglected in the derivation above.

Chapter 8

Photoionization in a laser pulse

For longer pulses and a range of characteristic parameters the integral (5.36) can be performed explicitly with the help of expansions into Bessel functions. This will allow us to derive the basic properties of photoelectron spectra in an alternative quantum mechanical context. It shows where and under which conditions peaks in the electron spectra appear separated by multiples of the fundamental laser frequency. This peak structure is popularly attributed to the discrete nature of "photons". However, it has no relation to the particle nature of light, it only reflects the periodicity of the field. Peaks in the electrons spectra are due to interferences due to the wave nature of electrons.

The scheme also allows to give a precise definition of the Keldysh parameter γ, which separates the regime where ionization is by multiphoton transitions from the regime of tunnel ionization.

8.1 Expansion into Bessel functions

We start from

$$b(\vec{k},t) = \int_{-\infty}^{t} dt' e^{i\Phi(\vec{k},t')} e^{-iE_0 t'} \vec{\mathcal{E}} \cdot \vec{d}[\vec{k} - \vec{A}(t')] \tag{8.1}$$

with the Volkov phase

$$\Phi(\vec{k},t') = \int_0^{t'} \frac{1}{2}[\vec{k} - \vec{A}(\tau)]^2 = \frac{1}{2}k^2 t' - \vec{k} \cdot \int_0^{t'} d\tau \vec{A}(\tau) + \frac{1}{2}\int_0^{t'} d\tau \vec{A}(\tau)^2. \tag{8.2}$$

We characterize a long pulse by the property

Slowly varying envelope

$$\vec{A}(t) = \vec{A}_0(t)\sin\omega t, \quad |\partial_t \vec{A}_0/\omega| \ll |\vec{A}_0|, \tag{8.3}$$

i.e. the envelope varies slowly on the scale of a single field oscillation. Under this condition the following approximations hold:

$$\vec{\mathcal{E}}(t) \approx -\partial_t \vec{A}(t) \approx \vec{\mathcal{E}}_0(t)\cos\omega t, \qquad \vec{\mathcal{E}}_0(t) := -\vec{A}_0(t)\omega \tag{8.4}$$

$$\int_0^{t'} d\tau \vec{A}(\tau) \approx -\frac{\vec{A}_0(t')}{\omega} \cos\omega t' \tag{8.5}$$

For the moment let us further assume that we are only interested in larger momenta

$$|\vec{k}| \gg |\vec{A}| \tag{8.6}$$

which allow the simplifying approximation

$$\frac{1}{2}[\vec{k} - \vec{A}]^2 \approx \frac{1}{2}k^2 - \vec{k}\cdot\vec{A}. \tag{8.7}$$

This approximation is only technical and will be removed below. Further we assume that the dipole matrix element is nearly constant over the momentum ranges covered by $\vec{A}(t)$

$$\vec{d}(\vec{k} - \vec{A}(t)) \approx \vec{d}(\vec{k}). \tag{8.8}$$

We obtain

$$b(\vec{k}, t) \approx \int_{-\infty}^{t} dt' e^{i\frac{1}{2}k^2 t' + \vec{k}\cdot\int_0^{t'} d\tau \vec{A}(\tau)} e^{-iE_0 t'} \vec{\mathcal{E}}\cdot\vec{d}(\vec{k}) \tag{8.9}$$

The integral over τ gives approximately, using (8.3)

$$\int_0^{t'} d\tau \left[k^2/2 + \vec{k}\cdot\vec{A}(\tau)\right] \approx \frac{k^2}{2}t' + \frac{\vec{k}\cdot\vec{A}_0(t')}{\omega}\cos\omega t', \tag{8.10}$$

which leads to

$$= \int_{-\infty}^{t} dt' e^{i\frac{1}{2}k^2 t' + i\frac{\vec{k}\cdot\vec{A}_0(t')}{\omega}\cos\omega t'} e^{-iE_0 t'} \frac{1}{2}\left[e^{i\omega t'} + e^{-i\omega t'}\right] \vec{\mathcal{E}}_0(t')\cdot\vec{d}(\vec{k}) \tag{8.11}$$

Now we use the expansion into Bessel functions

$$e^{iz\cos\omega t} = \sum_{n=-\infty}^{\infty} i^n J_n(z) e^{in\omega t} \tag{8.12}$$

to write (8.9) as a sum over Bessel functions

$$= \sum_{s=\pm 1}\sum_{n=-\infty}^{\infty} \int_{-\infty}^{t} dt' e^{it'\left[\frac{1}{2}k^2 - E_0 - (n+s)\omega\right]} i^n J_n\left(\frac{\vec{k}\cdot\vec{A}_0(t')}{\omega}\right) \frac{1}{2}\vec{\mathcal{E}}_0(t')\cdot\vec{d}(\vec{k}) \tag{8.13}$$

8.1.1 Single photon ionization

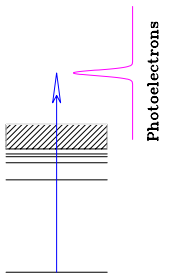

For single photon ionization we need rather high photon energies on the scale $\omega \sim 1$. Even at large laser intensities (e.g. $3 \times 10^{14} W/cm^2 \sim 10^{-2} a.u.$) this leads to very small arguments of the Bessel function

$$\frac{\vec{k} \cdot \vec{A}_0(t')}{\omega} \ll 1. \tag{8.14}$$

The Bessel functions for small arguments behave like

$$J_n(z) \approx \frac{z^n}{2^n} \frac{1}{n!}. \tag{8.15}$$

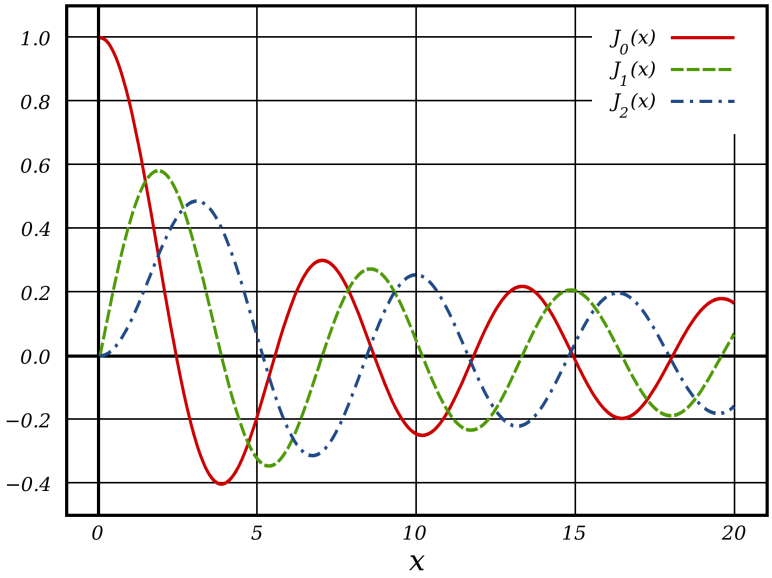

Figure 8.1: The Bessel functions (from Wikipedia).

At small arguments only $J_0 \approx 1$ contributes to the sum (8.13)

$$\approx \sum_{s=\pm 1} \int_{-\infty}^{t} dt' \underbrace{e^{it'\left[\frac{1}{2}k^2 - E_0 - s\omega\right]}}_{\text{rapidly oscill.}} \underbrace{J_0\left(\frac{\vec{k} \cdot \vec{A}_0(t')}{\omega}\right)}_{\approx 1} \underbrace{\frac{1}{2}\vec{\mathcal{E}}_0(t') \cdot \vec{d}(\vec{k})}_{\text{slow}} \tag{8.16}$$

The t'-dependence of $\vec{\mathcal{E}}_0(t')$ is much weaker than the oscillations of the phases $\exp[it'(k^2/2 - E_0 - s\omega)]$ everywhere except near

$$\frac{1}{2}k^2 \underbrace{-E_0}_{>0} - s\omega = 0. \tag{8.17}$$

What means "near" here depends on the variations of $\mathcal{E}(t')$. Condition (8.17) can only be fulfilled for $s = 1$ and we can drop the term $s = -1$, which leads to

$$\approx \int_{-\infty}^{t} dt' e^{it'\left[\frac{1}{2}k^2 - E_0 - \omega\right]} \frac{1}{2} \vec{\mathcal{E}}_0(t') \cdot \vec{d}(\vec{k}) \tag{8.18}$$

and finally to the single photon photoionization amplitude

$$b(k, t = \infty) = \frac{1}{2} \tilde{\vec{\mathcal{E}}}(\frac{1}{2}k^2 - E_0 - \omega) \cdot \vec{d}(\vec{k}). \tag{8.19}$$

The distribution of the electron energies is given as the Fourier transform of the pulse envelope $\mathcal{E}_0$

This is what is the meaning of the frequently heard statement of the kind "the photo electron pulse is a replica of the XUV pulse".

8.1.2 Hydrogen

The plane-wave dipole matrix element for the hydrogen ground state is according to Eq. (5.46).

$$d(\vec{k}) \propto \frac{k}{[1 + k^2]^3} \tag{8.20}$$

Integrating over 4pi angles and assuming $k_0 = \sqrt{2(\omega - E_0)} >> 1$ one obtains the total single-photon photoionization yield for Hydrogen as

$$\int d\varphi d\cos\theta k^2 b^2(\vec{k}) \sim k_0^2 \times (k_0^{-5})^2 \sim \omega^{-4} \tag{8.21}$$

Ionization rapidly decreases with increasing photon energy

As a rule, inner shell electrons are easier to XUV ionize than valence electrons, as their photo electron energy $k^2/2 = \sqrt{\omega - I_p}$ is lower.

The physical reason for this behavior is that the photon cannot give momentum to the electron, it must pick eletrons that already have the momentum. Fast moving electrons, however, occur only close to the nucleus where their higher kinetic energy is compensated by a large negative potential energy. The region shrinks with increasing momentum requirements.

For the same reason, XUV pulses directly probe only what happens very near to the nucleus. They are blind to what happens in the reginons, where, e.g., chemical binding happens.

Note:

Near threshold the plane wave dipole matrix element is incorrect. In the limit of $k \to 0$ the correct Coulomb matrix element remains finite, while the plane wave dipole goes to 0. The approximation remains rather poor in the range of $k \sim 1 - 2$, which happens to be the photoelectron momentum range in XUV photoionization with $\omega = 3$.

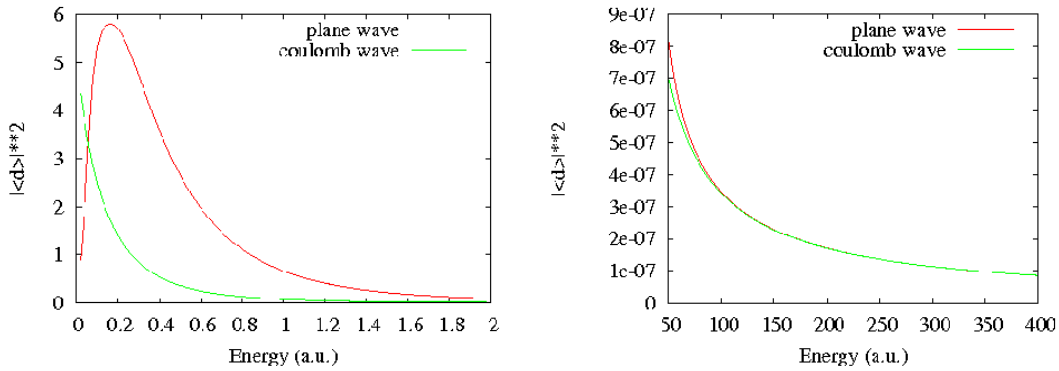

Figure 8.2: Plane wave (red) vs. correct Coulomb scattering wave (green) dipole matrix element squared. Lower and asymptotic energies.

8.2 Laser dressed photo-ionization

(go to RABITT section)

Typical values of $\vec{k} \cdot \vec{A}/\omega$

Krypton

8.2.1 Multi-photon emission, weak fields

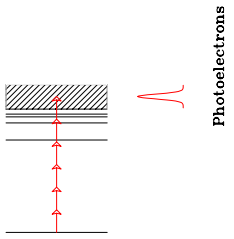

The integral is dominated by the rapidly oscillating phases $\exp\{it[\frac{k^2}{2} - E_0 - n\omega]\}$. Only momenta $\vec{k}$ contribute, where

$$k^2/2 - E_0 \approx n\omega \tag{8.22}$$

"n-photon electron emission"

As the left hand side is > 0 and ω is assumed to positive only *positive* n can fulfill this condition.

Suppose $\omega << |E_0|$ and $\vec{k} \cdot \vec{A}_0/\omega << 1$. In that case, the strongest contribution comes from the lowest n that can fulfill the condition (8.22), i.e. $n_0 > |E_0|/\omega$. The dependence

on the field strength is

$$b_{n_0}(\vec{k}) \sim \left(\frac{\vec{k}\cdot\vec{\mathcal{E}}_0}{\omega^2}\right)^{n_0} \tag{8.23}$$

Larger n contribute less by factors $(\vec{k}\cdot\vec{A}/\omega)^{(n-n_0)}$

Note: near to threshold the approximation of weakly $\vec{k}$-dependent $\vec{d}(\vec{k})$ usually fails. The statement above therefore only holds in an approximate sense. In general, the $\vec{k}$-dependence of $\vec{d}$ further enhances the lowest energy photons. In addition, for low energy electrons the approximation of neglecting $V_\perp$ is particularly serious, therefore the formula above is only qualitatively correct. This can be largely corrected by using more accurate dipole matrix elements.

8.2.2 Multi-photon emission, strong fields

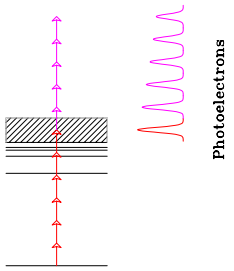

Suppose the field is strong: $\vec{k}\cdot\vec{A}/\omega \sim N$. The condition $\omega < |E_0|$ is not necessary, but it is usually fulfilled, as otherwise the first condition is hard to meet. Here we cannot neglect the A_0^2-term in the exponent, as A_0 may become of the same size or larger than the k that we look at.

The Volkov phase can be calculated in the approximation of a slowly varying A_0 as above to

$$\frac{1}{2}\int_t^0 d\tau k^2 + 2\vec{k}\cdot\vec{A}_0\cos\omega\tau + A_0^2\cos^2\omega\tau \approx -\frac{1}{2}t\left[k^2+\frac{1}{2}A_0^2\right] + \frac{\vec{k}\cdot\vec{A}_0}{\omega}\sin\omega t - \frac{A_0^2}{8\omega}\sin 2\omega t, \tag{8.24}$$

where we used $\cos^2\omega\tau = \frac{1}{2}[1+\cos 2\omega\tau]$.

After expansion into Bessel functions we obtain a double sum over integrals with rapidly oscillating terms

$$\sim \sum_{nm} e^{-it\left[\frac{1}{2}k^2+\frac{1}{4}A_0^2-\omega n-2\omega m\right]} J_n\left(\frac{\vec{k}\cdot\vec{A}_0}{\omega}\right) J_m\left(\frac{A_0^2}{8\omega}\right) \tag{8.25}$$

this does not work !

Now all $|n| \le |\frac{\vec{k}\cdot\vec{A}_0|}{\omega}$ and $|m| \le \frac{A_0^2}{8\omega}$ contribute comparably much. For larger n and m, the value of J_nJ_m rapidly drops off. The energy spectrum extends to

$$\frac{1}{2}k^2 + \frac{1}{4}A_0^2 - |E_0| = \vec{k}\cdot\vec{A}_0 + \frac{1}{4}A_0^2 \tag{8.26}$$

When E_0 is small compared to $\vec{k}\cdot\vec{A}_0$ this reduces to $(\vec{k}-\vec{A})^2 \approx 0$ or $k = A$. The maximal kinetic energy we see in the spectrum is

$$\frac{k^2_{\max}}{2} = \frac{A^2_{\max}}{2} = 2U_p \tag{8.27}$$

We have recovered the $2U_p$ cutoff of the classical model !

8.3 Tunneling vs.multi-photon regime

Suppose the field is weak and $|E_0| > \vec{k}\cdot\vec{A}_0$. We have the conditions

$$\omega n < \vec{k}\cdot\vec{A}_0 \tag{8.28}$$

and

$$\frac{k^2}{2} - E_0 \approx n\omega. \tag{8.29}$$

From that it follows that

$$k \approx A_0 \pm \sqrt{A_0^2 + 2E_0} \tag{8.30}$$

For

$$A_0 < |2E_0| \tag{8.31}$$

there are no real solutions for k. This defines the boundary between "tunneling" and "multi-photon" regime of photoionization. In the multi-photon regime $A_0 < |E_0|$ the arguments of the Bessel functions $\vec{k}\cdot\vec{A}_0$ are in the exponentially decaying part. In the tunneling regime, the values of the Bessel functions oscillate and are of order $O(1)$.

8.3.1 Keldysh parameter γ

The condition (8.31) can be written in the form

$$\gamma = \sqrt{\frac{2|E_0|}{A_0^2}} = \sqrt{\frac{|E_0|}{2U_p}} = \frac{\omega\sqrt{2|E_0|}}{\mathcal{E}_0} \tag{8.32}$$

$\gamma < 1$ ... "tunneling"
$\gamma > 1$ ... "multiphoton"

8.3.2 A popular interpretation of γ

$$\gamma \sim \frac{\text{tunneling time}\,\tau}{\text{optical period}\,T} \tag{8.33}$$

Tunneling time

— figure tunneling length —

Length of the tunnel:

$$l|\mathcal{E}| = |E_0|, \qquad l = \frac{|E_0|}{|\mathcal{E}|} \tag{8.34}$$

Velocity in the tunnel (?): = velocity in the bound state as obtained by the virial theorem

$$v_0 = \sqrt{2|E_0|} \tag{8.35}$$

Tunnel time:

$$\tau = \frac{l}{v_0} = \sqrt{\frac{|E_0|}{2}}\frac{1}{\mathcal{E}_0} \tag{8.36}$$

Optical period:

$$T = \frac{2\pi}{\omega} \tag{8.37}$$

It does not quite fit:

$$\frac{\tau}{T} = \frac{1}{4\pi}\gamma \tag{8.38}$$

8.3.3 A closer look at the Keldysh parameter

[L.V. Keldysh, Sov. Phys. JETP 20, 1307 (1965)]

Computes stationary photo-ionization rates in a CW field. The technique is what we know today as "strong field approximation".

We know our amplitudes at some time $b(\vec{k}, T)$ by SFA. The unbound part at T is

$$Y(T) = \int d^{(3)}k |b(\vec{k}, T)|^2 \tag{8.39}$$

If ever a stationary situation is reached, the yield will increase linearly in time. Obviously that cannot go on forever in reality because of depletion, but remember that we dropped depletion from our original version of the SFA. If there is any reasionable period of time where one sees a near linear increase of the yield, we can define a rate

$$w_0 := \lim_{T\to\infty}\frac{1}{T}Y(T) = \lim_{T\to\infty}\frac{1}{T}\int dk^{(3)}\left|\int_{-\infty}^{T} dt' e^{-i\Phi(\vec{k},T,t')-iE_0t'}\vec{\mathcal{E}}(t')\cdot\vec{d}[\vec{k}-\vec{A}(t')]\right|^2. \tag{8.40}$$

By construction, we have a time-periodic situation (CW field), therefore we can make a discrete Fourier expansion in the limit $T\to\infty$:

$$b(\vec{k}, T) = \sum_{n=-\infty}^{\infty}\int_0^T dt e^{i(\vec{k}^2+\vec{A}_0^2/4)t/2-iE_0t+in\omega t}L_n(\vec{k}) \overset{T\to\infty}{\longrightarrow} \sum_{n=-\infty}^{\infty}\delta(\frac{\vec{k}^2+\vec{A}_0^2}{2}-E_0-n\omega)L_n(\vec{k}) \tag{8.41}$$

The δ-functions are the infinite time limit of our ATI peaks. We also see that they are almost located where we expect them by the naive photo-ionization diagrams, *except* for a correction $\vec{A}_0^2/2$: This is the ponderomotive shift of the threshold, i.e. the photon-electron energy is decreased by the ponderomotive potential. Do we violate energy conservation? Is a non-integer number of photons absorbed?

Well, first of all, there are no "photons", the field is not quantized at all, we have just made a Fourier transformation. But secondly, no, we do not violate energy conservation even if we want to think in terms of photons: the energy is by construction in a CW field. If we gently switch it off, the photo-electron will be accelerated out of the field an gain exactly the missing energy of the ponderomotive potential $\vec{A}_0^2(\vec{r},t)/2$, where we must indicat the space-time dependence of the switch-off.

The Fourier components are (for notational simplicity $\vec{\mathcal{E}}_0 = (0,0,\mathcal{E}_0)$, $d[\ldots] := \vec{d}[\ldots]_z$):

$$L_n(\vec{k}) = \frac{\mathcal{E}_0}{2\pi}\int_{-\pi}^{\pi} dt' \exp\left[i\left(\frac{-\vec{k}\cdot\vec{A}_0}{\omega}\cos(\omega t') + \frac{\vec{A}_0^2}{8\omega}\sin(2\omega t') - n\omega t'\right)\right]\cos(\omega t')\vec{d}[\vec{k}-\vec{A}_0\sin(\omega t')] \tag{8.42}$$

We recognize our old friend the Bessel expansion in this integral, at least when we neglect the term $\propto \vec{A}_0^2$:

$$L_n(\vec{k}) \approx \frac{\mathcal{E}_0}{2\pi}\int_{-\pi}^{\pi} dt' \sum_m (-i)^m J_m(\frac{\vec{k}\cdot\vec{A}_0}{\omega}) e^{i(m-n)\omega t'}\cos(\omega t')\vec{d}[\vec{k}-\vec{A}_0\sin(\omega t')] \tag{8.43}$$

If we neglect the t'-dependence of $\vec{d}[\ldots]$, we see that the integral is proportional $J_{n\pm1}(\vec{k}\cdot\vec{A}_0/\omega)$. Note that due to the behaviour $J_n(z)\sim z^n$ starting from small $\vec{k}\cdot\vec{A}_0/\omega$, the Bessel functions vary exponentially with n starting from $\vec{k}\cdot\vec{A}_0/\omega \sim n$. What is the range where the argument is "small"? We may guess this, as the osciallation period of the Bessels appears to be approximately independent of n, the initial rise is $\propto n$, i.e. the behavior $\propto z^n$ breaks down near arguments $z\sim n$.

Remember that $k^2/2 = n\omega - |E_0|$. The transition from the ossillatory, weakly n-dependent behavior of $J_n(\vec{k}\cdot\vec{A}_0/\omega)$ to a power-law dependence $\sim(\vec{k}\cdot\vec{A}_0)^n$ occurs where

$$kA_0 = n_0\omega \quad \text{and} \quad k^2/2 = n_0\omega - |E_0| \tag{8.44}$$

$$\frac{n^2\omega^2}{2A_0^2} = n\omega - |E_0| \tag{8.45}$$

$$0 = \frac{n^2\omega^2}{2A_0^2} - n\omega + |E_0| \tag{8.46}$$

$$\tag{8.47}$$

Solve for n_0; for $\gamma = 1$ the discriminant becomes 0; i.e. for $\gamma > 1$ all contributions come from the osccilatore region of the Bessel functions.

The core of the Keldysh paper is about evaluating that sum. This is not done directly, but by going back to the original integral before expansion and doing a saddle point integration. With a few more approximations (probably not serious), one arrives at

$$w_0 = \dots \tag{8.48}$$

with the Keldysh parameter γ.

$$\gamma = \frac{\sqrt{-2E_0}}{|\vec{A}_0|} = \frac{\omega\sqrt{2I_p}}{\mathcal{E}_0} = \sqrt{\frac{I_p}{2U_p}} \tag{8.49}$$

There are two limiting cases: for $\gamma \ll 1$ many terms contribute to the sum over the Bessel functions and a typical tunneling type behavior of the field arises with an exponential dependence of the rate. In the converse case $\gamma \gg 1$, a multi-photon like behavior $\propto I^n$ arises.

8.3.4 ATI spectra

$$\frac{\vec{k}\cdot\vec{A}_0(t')}{\omega} \lesssim n_0 - 1 \tag{8.50}$$

$$b(\vec{k},t) = \int_{-\infty}^{t} dt' e^{i\Phi(\vec{k},t')}\chi(\vec{k},t') \tag{8.51}$$

$$\sum_{s=\pm1} e^{it'[E_0 - s\omega]}\frac{1}{2}\vec{\mathcal{E}}_0(t')\cdot\vec{d}(\vec{k}) \tag{8.52}$$

$$\approx \sum_{n=-\infty}^{\infty} J_n\left(\frac{\vec{k}\cdot\vec{A}_0(t')}{\omega}\right)\tilde{\chi}(\frac{1}{2}k^2 - n\omega) \tag{8.53}$$

$$\chi(t) = e^{-\frac{1}{2}\Gamma t}e^{-iE_0 t} \tag{8.54}$$

$$\int_0^\infty e^{-\frac{1}{2}\Gamma t}e^{-iE_0 t}e^{i\omega t} = \frac{i}{E_0 - i\Gamma/2 - \omega} \tag{8.55}$$

8.3.5 Angular streaking

Original proposal for the streaking measurements [Constant et al., PRA 1997]

Elliptic polarization: assuming peak emission at peak field (dominated by ellipticity), assuming free propagation after emission the peak momentum distribution can be predicted. If peak emission does not occur at peak field, an offset between expected and measure peak momentum would be observed. Needs correction for Coulomb field.

No serious delay observed.

But what is measured? In terms of the wave function, the electron is already "outside" the barrier, the field takes it from there "with no delay".

Classically, the particle must be inside the barier. If this were the case, indeed it would pass in "no time", or, more precisely, in less than 34 as. This, by the way, is just time time to proceed by 1.5 atomic units, indeed much shorter than the barrier thickness.

Conclusion (surprise): the particle does not travel through a long tunnel.

Chapter 9

Attosecond measurements

For measuring processes with attosecond duration, we need to be have a measurement instrument that we can control on an attosecond time scale and we need a process that ensures an effect of the measurement instrument on the measured phenomenon. For attosecond XUV pulses, a primary measurement tool would be the pulse itself — an autocorrelation measurement. However, as discussed, the interaction of XUV pulses with atoms is weak and higher order processes are difficult to detect. For the characterization of XUV pulses, the generating IR pulse is the perfect measurement tool: it is rigidly timed relative to the XUV time structure and delay lines allow precise control of the time delay. An it can be very strong such that two-photon processes become easily detectable, even if the XUV interaction is weak.

9.1 The attosecond streak camera

The RABITT method as described above is applicable only for pulse trains, as the spectral width of the harmonic peak must be smaller than the distance between peaks in order to be able to distinguish side-band from the original peaks. For single attosecond pulses this is no longer the case: an isolated pulse of, say, $150\,as$ has a continuous spectrum throughout its whole spectral width of $\sim 10\,eV$, which is much larger than $2\omega_l \sim 1.5\,eV$ (for 800 nm laser wave length). In this case, different methods are needed. The most successful of these methods is the "attosecond streak camera". Just like RABITT, the attosecond streak camera uses the cross-correlation of the laser field with the XUV field during XUV photo-ionization. Its basic physics is best understood in terms of classical physics.

Suppose an electron, treated as a classical particle, is released from an atom at a time t with an initial momentum $\vec{p}_i$ in the presence of a laser pulse with electric field $\vec{\mathcal{E}}(t)$. Between its release and detection the electron experiences a boost of

$$\Delta\vec{p} = -\int_t^\infty \vec{\mathcal{E}}(t')dt' = \vec{A}(t), \tag{9.1}$$

where have used $\vec{A}(\infty) = 0$. The momentum observed at the detector is then

$$\vec{p} = \vec{p}_i + \vec{A}(t). \tag{9.2}$$

Incidentally, $\vec{p}$ is the canonical momentum of the electron in velocity gauge, which is conserved during free propagation in the laser field. General wisdom has it, that a free electron cannot be accelerated by a laser pulse. Here, the at first sight surprising fact that a free electron is accelerated by a laser pulse arises, because the electron is set free *during* the laser pulse, *i.e.* it is *not* free during the whole pulse. If the electron were set free *before* the pulse, it would indeed not be accelerated as $\vec{A}(-\infty) = \int_{-\infty}^{\infty} \vec{\mathcal{E}}(t)dt = 0$ for a freely propagating laser pulse.

If electrons are released during an extended period of time the *time distribution* of the release process is mapped into a *momentum distribution* of the measured electrons, as illustrated in Fig. 9.1 for a linearly polarized streak field with $\vec{p}_i \parallel \vec{A}(t)$. This is the basic principle of the attosecond streaking measurement.

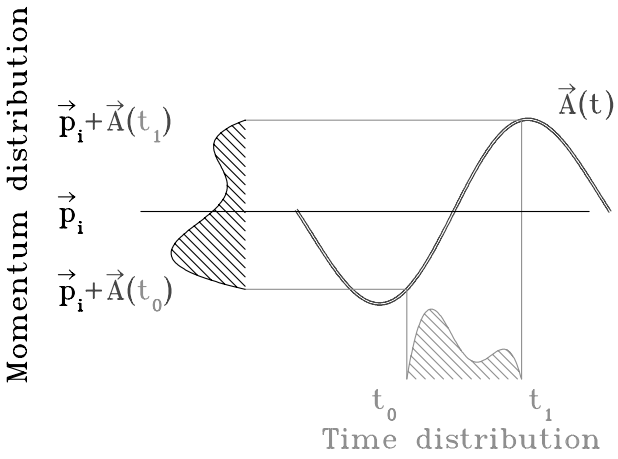

Figure 9.1: Mapping time-distributions into momentum distributions. Electrons are released between times t_0 and t_1 with a certain time-dependent intensity profile and constant initial momentum $\vec{p}_i$. The laser field with vector potential $\vec{A}(t)$ shifts the momenta to different final momenta $\vec{p} = \vec{p}_i + \vec{A}(t)$, depending on the release time t. For clarity, it is assumed $\vec{p} \parallel \vec{A}(t)\, \forall t$.

9.1.1 The experimental setup

9.1.2 Geometric effects in streaking measurements

The principle laid out above for the case $\vec{p} \parallel \vec{A}$ can be readily generalized to other experimental geometries. For example, in the first streaking measurements [5, 4] electrons were detected perpendicular to the laser polarization direction. As in that case not only the magnitude of the emitted electron momentum is changed, but also its direction, effects of the measurement geometry are superimposed on the simple boosting picture explained

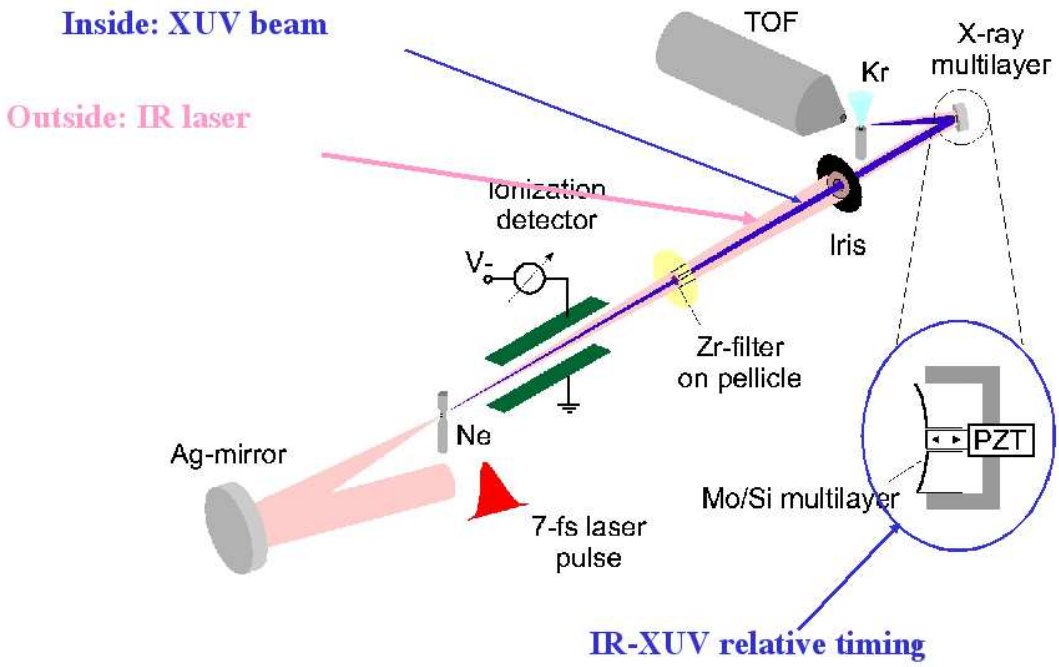

Figure 9.2: Experimental setup for the attosecond streaking measurements. An IR laser is focused into a gas jet, where it generates a harmonic pulse. IR and harmonic are accurately time-locked. A filter blocks the laser in the central part of the beam. The beam is focused by a mirror, whose inner part is movable and carries a multi-layer mirror designed to filter the high harmonics. Time-delay between IR and XUV is controlled by the variation of the path length of the two parts of the beam. In the focus of the beams photoelectrons are produced and detected by time-of-flight (Figure from Drescher et al.[4]).

above. If one assumes (as in photoionization), a rather well defined initial photoelectron energy E_i, the momenta of all emitted electrons lie on a sphere in momentum space with radius $\sqrt{2mE_i}$. Streaking shifts this sphere as a whole by $\vec{A}(t_i)$, leading to maximum acceleration in forward direction and maximum deceleration in backward direction. In the perpendicular direction the effect of the boost is minimal of the order $\sim |\vec{A}(t)|^2$ if $E_i \gg |\vec{A}(t)|^2$. When, as in any experiment, electrons are collected from a finite opening angle, a *geometrical broadening* of the detected electron spectrum occurs, even when the unidirectional spectrum is not broadened. The effect is weakest parallel to the laser polarization and maximal in perpendicular direction (c.f. Fig. 9.3). Provided the measurement geometry is well known, these geometrical effects can be easily corrected for. We will therefore disregard all geometrical effects in the further discussion and concentrate on the case $\vec{p} \parallel \vec{A}$.

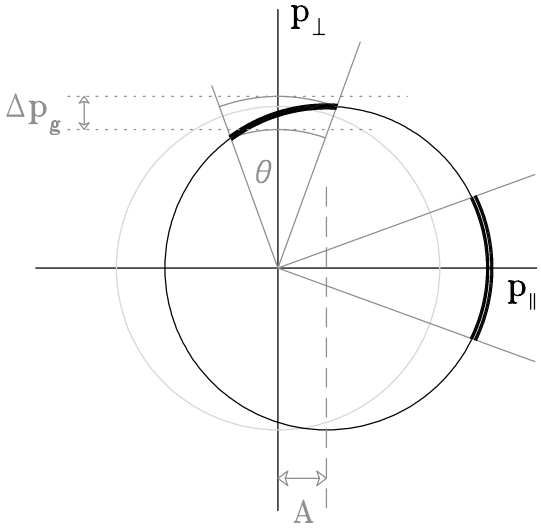

Figure 9.3: Geometric effects in a streaking measurement. Streaking shifts the circle corresponding to equal emission energies (light grey) in momentum space by $\vec{A}$ to a circle of observed momenta (black). Parallel to the laser field polarization, the electron energies are maximally boosted. In perpendicular direction the boost is much smaller, but when collecting electrons over a finite angle θ, the momentum spectra experience a purely geometrical broadening by Δp_g.

9.1.3 Separating laser-ATI from XUV-photoelectrons

The maximum streaking laser field is limited by the requirement that the unavoidable photoionization by the laser (ATI electrons) remains energetically separate from the streaked XUV photoelectrons. A simple estimate can be made in terms of classical mechanics.

Maximal ATI energy (direct electrons)

$$P_{ATI} = \sqrt{2(2U_p)} = |\vec{A}_{max}| \tag{9.3}$$

Lower edge of the streaked XUV photo-electron spectrum

$$P_X = \sqrt{2(\omega_{XUV} - I_p)} - |\vec{A}_{max}| \tag{9.4}$$

From

$$P_{ATI} < P_X \tag{9.5}$$

it follows

$$\boxed{4U_p < \omega_{XUV}}$$

Note: The problem is smaller for observation direction $\perp$ to laser polarization for two reasons: the momentum shift due to streaking is smaller (cf. Fig. 9.3) and the ATI

photo-electron momenta perpendicular to laser polarization are smaller.

9.1.4 Measuring the chirp

This simple classical picture of streaking also allows to see, how the chirp (linear) frequency chirp of the attosecond pulse can be measured. Chirp means that the frequency, e.g., increases from red to blue during the pulse. This means that early photoelectrons will have lower energies than later ones, i.e. the initial momentum becomes time-dependent $\vec{p}_i(t)$. Depending on how the laser vector potential changes during the XUV pulse, the variation of $\vec{p}_i(t)$ over the XUV pulse can either be further enhanced or reduced by laser-field acceleration. By comparing the broadening of the streaked photo-electron spectra measured with two different IR-XUV time-delays one detects a possible chirp in the pulse. Note that — as expected by theory — pulses from cutoff harmonics have very little chirp.

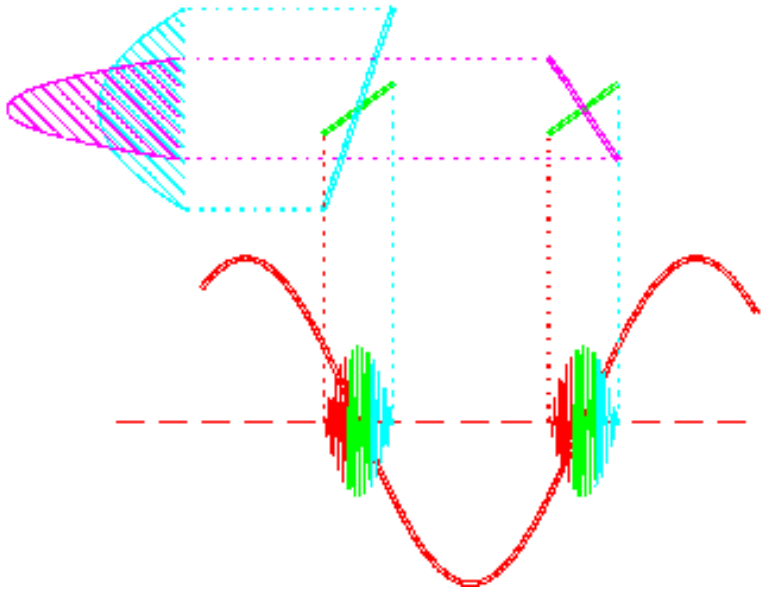

Figure 9.4: Detecting chirp in an XUV pulse by making measurements at two different time-delays at two subsequent nodes of the vector potential (corresponding to two subsequent peaks of the laser field). The time-dependence of the initial photo-electron momentum due to the chirp is indicated by the shorter sloped line, which is equal for both measurements. Acceleration by the IR field enhances or reduces the initial slope, leading to smaller or narrower photo-electron spectra.

9.2 Trains of attosecond pulses

Trains of attosecond pulses are generated by *long* laser pulses. High harmonics are generated by recollision. In the case of a long laser pulse, the time structure of harmonic

emission is (nearly) periodic with half the period of the laser field $T/2$. The period is $T/2$, because harmonic emission is equal for negative and positive electric fields.

The power spectrum therefore has sharp (δ-like) peaks that are separated by $2\omega_l = 2\pi/(T_l/2)$. The first peak in this series is the peak at the fundamental frequency ω_l, the further peaks therefore are at *odd* multiples of ω_l.

When harmonic emission is not strictly periodic with $T_l/2$, additional frequencies may show up. When the medium is not inversion symmetric, positive and negative fields can produce different harmonic response. In that case, the period of harmonic emission is T_l and consequently peaks in the power spectrum are separated by $\omega_l = 2\pi/T_l$.

In anisotropic media *even* harmonics may be generated

Note: When pulses become very short, the pulse itself may no longer be reflection symmetric and therefore "even harmonics", or, more accurately structures that are not at multiples of the fundamental frequency may appear.

9.2.1 Relation between time structure and power spectrum

The higher harmonic electric field is

$$\mathcal{E}(t) = Re \sum_{m>1}^{\infty} e^{im\omega_l t} |a_m^2|^{1/2} e^{i\varphi_m} \tag{9.6}$$

The power spectrum $|a_m^2|$ of the harmonics can be measured easily. For the *time structure* we need to know the phases: the phases determine, how the individual terms in the sum interfere, constructively or destructively (or anything in between). By time structure we mean the average power in the field, where averaging is over at least one optical cycle of the lowest frequency involved.

Note: An overall constant phase shift $\varphi_m \to \varphi_m + \Delta\varphi_0$ does not change the time structure.

Note: A time-shift $t \to t + \Delta t$ changes the difference between φ_m and φ_{m+1} by

$$\Delta\varphi_m = \varphi_{m+1} - \varphi_m = \omega_l \Delta t \tag{9.7}$$

That is, a constant phase-shift between harmonics which corresponds to a a phase that changes linearly with the harmonic number n only shifts the pulse in time, but does not change its time structure. We conclude:

For the determination of the time structure of the harmonic radiation we need to know the change of phase differences of subsequent harmonics, i.e. the second difference of the phase $\Delta^{(2)}\varphi_m = \Delta\varphi_{m+1} - \Delta\varphi_m = \varphi_{m+1} - 2\varphi_m + \varphi_{m-1}$ (9.8)

9.2.2 RABITT — Measurement of $\Delta\varphi_m$

The acronym "RABITT" stands for "Reconstruction of Attosecond Beating by Interference of Two-photon Transitions" this acronym was to my knowledge invented by Harm Muller, but the method was actually proposed by Veniard et al. [17]. The two-photon transitions in the acronym refer to two-color IR-XUV photoionization, where an XUV pulse train produces a series of single photon peaks at photo-electron energies $(2m+1)\omega_l - I_p$ and the simultaneously present laser pulse produces side-bands in the center between the peaks at $(2m+1)\omega_l - I_p \pm \omega_l$. We will see below, that the amplitude of the side-bands contains information about the relative phases of the harmonic frequencies.

Laser-dressed photoionization by high harmonics

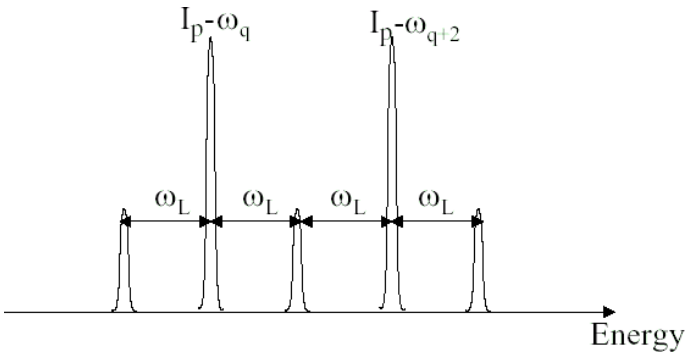

Figure 9.5: Photo-electron spectrum generated by a high harmonic radiation plus the fundamental laser field. Between the photo-ionization peaks corresponding to odd multiples of the laser frequency ω_l extra peaks appear due to two-photon processes.

9.2.3 Laser dressed photoionization

For now, we assume infinite pulse trains of the harmonic radiation, which can be written as the sum over their spectral components $\mathcal{E}_{XUV}(t) = \sum_m \mathcal{E}_{2m+1}(t)$ with

$$\mathcal{E}_{2m+1}(t) = \mathcal{E}_{2m+1}\cos[(2m+1)\omega_l t + \varphi_{2m+1}] \tag{9.9}$$

and a CW laser field

$$\mathcal{E}_1(t) = \mathcal{E}_1\cos[\omega_l t + \omega_l \Delta t] = \mathcal{E}_1\cos[\omega_l t + \varphi_1], \tag{9.10}$$

whose time delay Δt relative to the harmonic pulse can be varied.

According to Eq. (5.36), the photo-electron amplitude generated by a train of pulses composed of odd $(q = 2m+1)$ harmonics in a dressing laser field is given by

$$b(\vec{k}) = \int_{-\infty}^{\infty} dt e^{\frac{i}{2}\int_{-\infty}^{t}\{\vec{k}+\vec{\mathcal{E}}_1/\omega_l\cos[\omega_l(\tau+\Delta t)]\}^2 d\tau - iE_0 t}\sum_{m=0}^{\infty}\vec{d}\cdot\vec{\mathcal{E}}_{2m+1}\cos[(2m+1)\omega_l t + \varphi_{2m+1}] \tag{9.11}$$

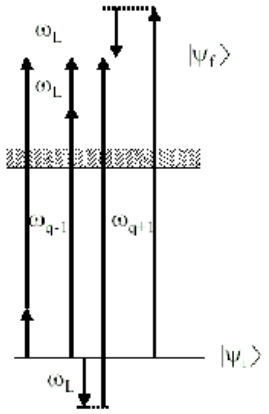

Figure 9.6: Scheme of the IR-XUV two-photon ionization that generates to photo-electron energies $(2m+1)\omega_l - I_p$. For each such peak, there are 4 alternate paths as indicated. Interference between these paths makes the process sensitive to the relative phases.

Approximations

- neglect $\mathcal{E}_1$ in the dipole transition: We assume that the laser frequency is too low to generate single-photon transitions and we assume that the laser field is too weak to cause *multi*-photon transitions.
- neglect $\mathcal{E}_{2m+1}/[(2m+1)\omega]$ in the Volkov phase: $\mathcal{E}_{2m+1} \ll \mathcal{E}_1$ and $m >> 1$. weaker than the laser field and its impact is further reduced by the higher frequency that appears in the denominator: the harmonic vector potential is much smaller . This is the same approximation that we made when we kept only the $J_{n=0}$ terms for single photon ionization.

Calculation steps

Expand the $\cos[\omega_l(t+\Delta t)]$-term of the Volkov phase into Bessel functions

$$\begin{aligned}
&\int_{-\infty}^{\infty} dt \sum_m e^{i\int_0^t \vec{k}^2/2 + \vec{\mathcal{E}}_1/\omega_l \cos[\omega_l(t+\Delta t)]d\tau - iE_0 t} \vec{d}\cdot\vec{\mathcal{E}}_{2m+1} \cos[(2m+1)\omega_l t + \varphi_{2m+1}] \\
&\approx \sum_m \int_{-\infty}^{\infty} dt \quad e^{\frac{i}{2}\int_{-\infty}^t k^2 d\tau - iE_0 t} \\
&\quad \sum_{n=-\infty}^{\infty} i^n J_n\left(\frac{\vec{k}\cdot\vec{\mathcal{E}}_1}{\omega_l^2}\right) e^{in[\omega_l(t+\Delta t-\pi/2)]} \times \vec{d}\cdot\vec{\mathcal{E}}_{2m+1} \frac{i}{2} \sum_{s=\pm 1} s e^{si[(2m+1)\omega_l t + \varphi_{2m+1}]}. \quad (9.12)
\end{aligned}$$

Here we have neglected the terms containing $\vec{\mathcal{E}}_1^2$. We assume that the laser field is weak after all, *i.e.* the argument in the Bessel function remains < 1. Then we may keep only

the lowest contributions from the exponents $n = 0, \pm 1$:

$$\begin{aligned} \approx & \int_{-\infty}^{\infty} dt \sum_m \sum_{n=-1}^{1} \sum_{s=\pm 1} \frac{i}{2} J_n \left(\frac{\vec{k} \cdot \vec{\mathcal{E}}_1}{\omega_l^2} \right) \vec{d} \cdot \vec{\mathcal{E}}_{2m+1} \\ & \times s \exp \left\{ \frac{i}{2} \int_{-\infty}^{t} k^2 d\tau - iE_0 t + in[\omega_l (t + \Delta t)] + si[(2m+1)\omega_l t + \varphi_{2m+1}] \right\}. \end{aligned} \tag{9.13}$$

We see again the appearance of rapidly oscillating phases. For $J_{n=0}$ these have stationary points only at the photo-electron energies $k^2/2 = (2m+1)\omega_l + E_0$. The terms $J_{n=\pm 1}$ give contributions to the side-band peaks at $k^2/2 = 2m\omega_l - E_0$. To a given side-band peak $2m$ we have contributions from harmonic $2m+1$ in combination with the Bessel factor $J_{n=-1}$ and from harmonic $2m-1$ with $J_{n=+1}$. Keeping only these terms and neglecting the "counter-rotating" contribution $s = 1$, we obtain

$$\begin{aligned} \approx & \frac{1}{2} \int_{-\infty}^{\infty} dt \\ & \left[\vec{d} \cdot \vec{\mathcal{E}}_{2m+1} \int_{-\infty}^{\infty} dt e^{\frac{i}{2}\int_{-\infty}^{t} k^2 d\tau} J_{-1} \left(\frac{\vec{k} \cdot \vec{\mathcal{E}}_1}{\omega_l^2} \right) e^{i[2m\omega_l t + \varphi_{2m+1} - \omega_l \Delta t]} \right. \\ & \left. - \vec{d} \cdot \vec{\mathcal{E}}_{2m-1} \int_{-\infty}^{\infty} dt e^{\frac{i}{2}\int_{-\infty}^{t} k^2 d\tau} J_1 \left(\frac{\vec{k} \cdot \vec{\mathcal{E}}_1}{\omega_l^2} \right) e^{i[2m\omega_l t + \varphi_{2m-1} + \omega_l \Delta t]} \right] \end{aligned} \tag{9.14}$$

Observing that $J_{-1}(x) = -J_1(x)$ we obtain the side-band amplitude

$$\begin{aligned} b_{2m}(\vec{k}) \propto & \frac{1}{2} J_1 \left(\frac{\vec{k} \cdot \vec{\mathcal{E}}_1}{\omega_l^2} \right) \\ & \left[\vec{d}(\vec{k}) \cdot \tilde{\vec{\mathcal{E}}}_{2m+1} (\frac{\vec{k}^2}{2} - E_0 - 2n\omega_l) e^{i(\varphi_{2m+1} - \omega_l \Delta t)} \right. \\ & \left. + \vec{d}(\vec{k}) \cdot \tilde{\vec{\mathcal{E}}}_{2m-1} (\frac{\vec{k}^2}{2} - E_0 - 2n\omega_l) e^{i(\varphi_{2m-1} + \omega_l \Delta t)} \right] \end{aligned} \tag{9.15}$$

The modulus squared of this amplitude, *i.e.* the height of the side-band peak consists of a constant term plus a term that oscillates with the delay time Δt at twice the laser period:

$$\boxed{|b_{2m}|^2 \propto \cos(\varphi_{2m+1} - \varphi_{2m-1} + 2\omega_l \Delta t + \phi_a(\vec{k}_m)) + \text{const.}}$$

Here ϕ_a is an "atomic" phase from the $\vec{k}$-dependence of the dipole element $\vec{d}(\vec{k})$. Its variation with electron momentum can be determined reliably from theory. The phase-offset of the beats of subsequent side-band peaks with the laser delay time, gives the second differences

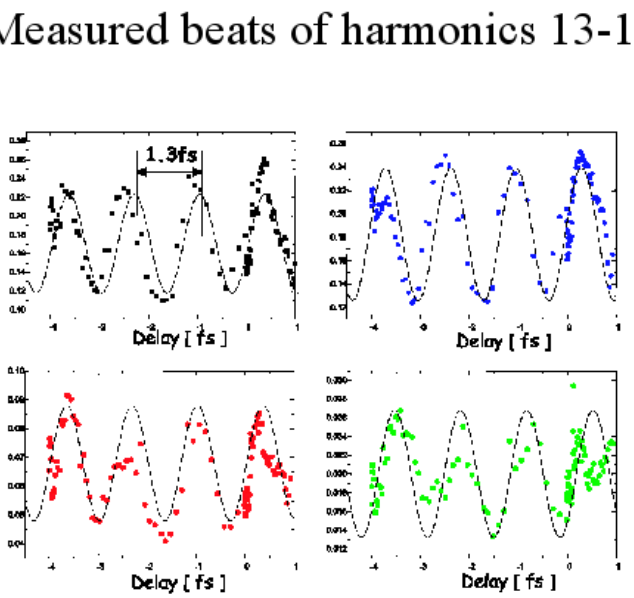

Figure 9.7: Beats of the side-band peak amplitudes with the IR-XUV delay time Δt. From the *offset* of the beats of side-bands $2m\omega_l$ and $(2m+2)\omega_l$ and the second phase differences $\Delta^{(2)}\varphi_m$ can be determined (Figure taken from Paul *et al.* [11]).

9.2.4 The quantum description of streaking

For low laser intensities we can use the exactly same derivation that has lead us to Eq. (9.15). The difference is,

(1) we have only a single photoelectron line around the central frequency of the XUV pulse $(2m+1)\omega_l = \omega_X$ and

(2) that line is much broader that the laser photon, because the XUV pulse is short compared to the laser period with a pulse envelope $\mathcal{E}_{2m+1} \to \mathcal{E}_X(t)$.

This reduces the sum (9.13) to

$$\begin{aligned} \approx & \int_{-\infty}^{\infty} dt \sum_{n=-1}^{1} \frac{i}{2} J_n\left(\frac{\vec{k}\cdot\vec{\mathcal{E}}_1}{\omega_l^2}\right) \vec{d}\cdot\vec{\mathcal{E}}_X(t) \\ & \times \exp\left\{\frac{i}{2}\int_{-\infty}^{t} k^2 d\tau - iE_0 t + in\omega_l(t+\Delta t) - i\omega_X t\right\}, \end{aligned} \tag{9.16}$$

where we have already made the rotating wave approximation for the XUV carrier. Now taking the integral over time, we obtain as for Eq. (9.15)

$$\begin{aligned} b(\vec{k}) \propto \quad & J_0\left(\tfrac{\vec{k}\cdot\vec{\mathcal{E}}_1}{\omega_l^2}\right) \quad \vec{d}(\vec{k})\cdot\tilde{\vec{\mathcal{E}}}_X(\frac{\vec{k}^2}{2}-E_0-\omega_X) \\ & +J_1\left(\tfrac{\vec{k}\cdot\vec{\mathcal{E}}_1}{\omega_l^2}\right) \quad \Big[\vec{d}(\vec{k})\cdot\tilde{\vec{\mathcal{E}}}_X(\frac{\vec{k}^2}{2}-E_0-\omega_X-\omega_l)e^{-i\omega_l\Delta t} \\ & \qquad +\vec{d}(\vec{k})\cdot\tilde{\vec{\mathcal{E}}}_X(\frac{\vec{k}^2}{2}-E_0-\omega_X+\omega_l)e^{i\omega_l\Delta t}\Big] \end{aligned} \tag{9.17}$$

For pulse shorter than the laser optical period, the three J_n-components (n=-1,0,1) that dominate the effect at lower laser amplitudes overlap and interfere. Interference depends on the relative phases of the contributions which vary with the time-delay Δt. Assume we have at time-delay $\Delta t = 0$ constructive interference of the lower energy component with the central component but destructive interference at the higher energy component. This will shift the overall peak to lower energies. At a time-delay $\omega_l\Delta t = \pi$ the situation reverses: now we have constructive interference at higher energies and a corresponding shift of the overall photo-electron peak to higher energies: the streaking shift has happened.

9.2.5 A unified description of attosecond-infrared cross-correlation

Both, the streak-camera and RABITT are based on the same physical process, *i.e.* on the modulation of XUV photo-electron spectra by a dressing laser field. They differ only in the range parameters, where they are applied. In fact, the analysis of both types of measurements is based on the same theoretical picture, *viz.* on the SFA (see section 5.3.1). We have derived Eq. (5.3.1) for the electron spectral amplitude in SFA. The measured spectra as a function of IR-XUV time delay Δt are given by modulus squared of the amplitude

$$\sigma(\vec{k},\Delta t) = |b(\vec{k},t=\infty)|^2 = \left|\int_{-\infty}^{\infty} dt' e^{i\Phi(\vec{k},t',\vec{A}_{IR})-iE_0t'}\vec{\mathcal{E}}_{XUV}(t'-\Delta t)\cdot\vec{d}[\vec{k}-\vec{A}_{IR}(t')]\right|^2 . \tag{9.18}$$

Here we have made the same approximations as in section (9.2.2): we have neglected the influence of the XUV field on the Volkov phase Φ and we have neglected ionization by the infrared field. In fact, both types of XUV pulse measurements discussed above are correctly described by this formula.

For the streaking measurement, it is easy to believe that we can extract the IR vector potential from a series of spectra without knowing much about the XUV pulse. Once we know the IR field, we can extract XUV pulse duration and chirp from the same data, and in an iterative procedure both fields can be reconstructed from the same measurement. Less obviously, the same holds for RABITT. How does this work?

Let us pause for a moment and have a look at this equation: on the left hand side, we have a function of a 3d continuous vector $\vec{k}$ and the continuous variable Δt. In an ideal measurement of the complete electron spectrum, we would have a dense set of data in a

4-dimensional space. On the right hand side, we have essentially two unknown functions of time $\vec{\mathcal{E}_{XUV}}(t)$ and $\vec{A}_{IR}(t)$. For simplicity, we assume here that the dipole moment $\vec{d}(\vec{k})$ is reliably known from other sources, theory or measurement. It looks like we are measuring a lot more data than what we need! Imagine, for example, we had two vectors for a dense set of sampling times t_i of values of the XUV $\mathcal{E}_{XUV}(t_i)$ and infrared $\mathcal{E}_{IR}(t_j)$ fields. But we measure a whole matrix of spectral values $\sigma(\vec{k}_n, \Delta t_l)$, surely containing a lot more information than just two vectors.

This redundancy can be exploited to reduce experimental errors. It was noticed in Ref. [9] that Eq. (9.18) has the general shape of a phase-gate version of the Frequency Resolved Optical Gating (FROG) technique for measuring short pulses [1]. Elaborate codes and algorithms for the optimal reconstruction of both, the phase gate function $\vec{A}_I R$ and the XUV field $\mathcal{E}_{XUV}$ are available for FROG-type measurements [15]

This unites the streaking and RABITT type measurements as extreme cases of the same single measurement method.

Literature

The basic idea for RABITT was published by Veniard *et al.* in 1996 [17], it was applied for the first proof of attosecond time structure in pulse trains by Paul *et al.* [11]. The name RABITT "Reconstruction Attosecond harmonica Beating by Interference of Two-photon Transitions" was invented by H. Muller [10]

The original proposal for the attosecond streak camera was by Constant *et al.* (1997) [3]. There it was suggested to use circularly polarized laser fields and observe the angular distribution of the XUV photoelectrons. The quantum theory was published in 2002 by Kitzler *et al.* [7] and Itatani *et al.* [6].

[1] Actually, there are two minor differences to the FROG phase gate: (1) the Volkov phase Φ depends on $\vec{k} \cdot \int dt' \vec{A}(t')$ *and* on $\int dt' \vec{A}^2(t')$, but in most cases the influence of the second term can be neglected; (2) $\vec{A}$ also appears in the dipole matrix element, again the influence of this can be neglected in the applications discussed here.

9.3 HHG from CO_2

9.3.1 The physical idea

Lein, M. et al. Role of the intermolecular phase in high harmonic generation. Phys. Rev. Lett. 88, 183903 (2002).

At fixed internuclear axis, the harmonic generation process at the different centers of the may lead to interference.

Phase difference of the dipole matrix from two sources separated by $\vec{a}$, assuming the wave electronic wave function at both centers is identical.

$$\langle \vec{k}|r|\phi(\vec{r}+\vec{a})\rangle = e^{-i\vec{k}\vec{a}}\langle \vec{k}|r|\phi(\vec{r})\rangle \tag{9.19}$$

For $\vec{k}\vec{a} = \pi$ destructive interference. Indeed, such a minimum was found!

The story, however, may not always be as simple as it looks here: a full numerical simulation of H_2 does not seem to reproduce the behavior that would be expected for photo-electron spectra by a similar interference mechanism [Y.V.Vanne, A. Saenz PRA 82, 11404(R), (2010)].

9.3.2 Experimental findings

Kanai, T., Minemoto, S. & Sakai, H. Quantum interference during high-order harmonic generation from aligned molecules. Nature 435, 470474 (2005).

Vozzi, C. et al. Controlling two-center interference in molecular high harmonic generation. Phys. Rev. Lett. 95, 153902 (2005).

Boutu, W. et al. Coherent control of attosecond emission from aligned molecules. Nature Phys. 4, 545549 (2008).

Zhou, X. et al. Molecular recollision interferometry in high harmonic generation. Phys. Rev. Lett. 100, 073902 (2008).

In hindsight: intensity dependence due to participation of different orbitals, not only the "highest occupied orbital" (HOMO).

9.3.3 The model

[O. Smirnova et al., Nature 460, 972 (2009)]: the main idea is that not only the least bound electron may contribute to HHG. As emission depends also on the symmetry of the orbital, for certain orientations of the molecular axis relative to polarization direction, deeper bound orbitals may contribute more to HHG then the least bound one.

The model is build basically from the pieces we have learnt: SFA, dipole matrix elements, quasi-classical propagation. New additions are some quantum chemistry and a correction for the propagation in the molecular potential.

For the purposes here, we assume the nuclei to be fixed at their positions, which is OK for the rather heavy C and O nuclei. Even for protons, typical velocities are ~ 11 fs, the time-scales decrease linearly with increasing mass.

In simplest (Hartree-Fock) approximation, we can consider the electronic wave function as the anti-symmtrized product of single-electron orbitals

$$\Psi_n(\vec{r}_1, \ldots \vec{r}_N) \approx \mathcal{A}\phi_1(\vec{r}_1) \ldots \phi_{N-2}(\vec{r}_{N-2})\phi_{N-1}(\vec{r}_{N-1})\phi_N(\vec{r}_N) \tag{9.20}$$

For simplicity we will drop in the anti-symmetrization operator $\mathcal{A}$ from here on. We assume here the individual "orbitals" ϕ_j to be associated with a ionization potential E_j, and let the numbering such that ionization potential decreases with j. We call ϕ_N the "highest occupied orbital" (HOMO). Clearly, quasi-static tunneling ionization will prefer to take the electron from the most weakly bound orbital E_N. However, for directions of the field in some nodal plane of the orbital ϕ_N, ionization may be strongly suppressed. In that case, ionization from the "HOMO-1" ϕ_{N-1} may compete with or exceed ionization from ϕ_N.

A few notes of caution:

- Quantitatively we need at present to rely on molecular ADK for ionization form an individual orbital. Compare for this the simple 2d study on molecular ADK and limitations of its accurcacy.

- The Hartree-Fock picture of electronic structure is a brutal simplification of the actual electronic structure. It discards all "correlation" of the electrons. The importance correlation for ionization is inknown.

- Any HF wave function will be rather poor at larger distances from the nuclei, as it is obtained by optimization the *energy* of the electrons, to which the tails of the wave function contribute rather little. This holds more generally for wave functions from quantum chemistry calculations. Technically, quantum chemistry wave fuctions are based on Gaussians, which have the wrong long-range behavior $\exp[-ar^2]$ rather than $\exp[-br]$.

- The problems can be partially controlled by using the Dyson orbitals (see below).

A very naiv picture of ionization would be to remove one of the orbitals from the determinant, thus obtaining the ionic wave functions

$$\begin{aligned}
\Phi^{(0)} &= \mathcal{A}\phi_1(\vec{r}_1) \ldots \phi_{N-2}(\vec{r}_{N-2})\phi_{N-1}(\vec{r}_{N-1} && (9.21)\\
\Phi^{(-1)} &= \mathcal{A}\phi_1(\vec{r}_1) \ldots \phi_{N-2}(\vec{r}_{N-2})\phi_N(\vec{r}_N) && (9.22)\\
\Phi^{(-2)} &= \mathcal{A}\phi_1(\vec{r}_1) \ldots \phi_{N-1}(\vec{r}_{N-1})\phi_N(\vec{r}_N) && (9.23)\\
&\vdots && (9.24)
\end{aligned}$$

Note that the use of product states for neutral and ion illustrates the idea, but is not essential at this point.

The states of unbound system we approximate as products of the ionic states with Volkov states as

$$\Psi_{scatter} \approx |\Phi^{(-j)}\rangle|\vec{k}, t\rangle \tag{9.25}$$

As before, the plane wave approximation for $|\vec{k},t\rangle$ is a serious one. Also, as an additinional approximation in the multi-particle case, *correlation* between the bound and scattering electrons is neglected: the approximation in the multi-electron case is even cruder than for a single electron.

In the spirit of the SFA and assuming that HOMO and HOMO-1 contribute, the ansatz for the total wave function in field is

$$|\Psi_{total}(t)\rangle = c(t)|\Psi_n\rangle_N + \int d^{(3)}k|\Phi^{(0)}\rangle|\vec{k},t\rangle b^{(0)}(\vec{k},t) + |\Phi^{(-1)}\rangle|\vec{k},t\rangle b^{(-1)}(\vec{k},t) \tag{9.26}$$

and using the same reasoning as in the single-electron case we find

$$b^{-j}(\vec{k},t) = \int_0^t dt' \,\langle\Phi^{(-j)}|\langle\vec{k},t|U(t,t')\vec{\mathcal{E}}(t')\vec{r}U_0(t',0)|\Psi_n\rangle \tag{9.27}$$

The error that we have made so far is that we use the simple product states (9.25) instead of the exact scattering states.

The field-free time-evolution is simply

$$U_0(t',0)|\Psi_n\rangle = e^{-itE_n}|\Psi_n\rangle. \tag{9.28}$$

We approximate the full time evolution as

$$U(t,t') \approx U_i(t,t') \otimes U_V(t,t') \tag{9.29}$$

with the ionic time-evolution further simplified as

$$U_i(t,t') \approx \sum_j |\Phi^{(-j)}\rangle e^{-i(t-t')E_j}\langle\Phi^{(-j)}| \tag{9.30}$$

i.e. we assume that the field does not affect the ionic states and they just evolve according to their eigenenergies. The unbound electron undergoes a Volkov evolution U_V like in the single electron case.

The important point about this particularly simple ansatz is that the ionic states do not get mixed by the field. As a result, when we insert the approximations, we obtain

$$b^{-j}(\vec{k},t) = \int_0^t dt' \, e^{-i(E_n-E_j)(t-t')}e^{-i\Phi(\vec{k},t,t')}\langle\Phi^{(-j)}|\langle\vec{k},t|\vec{r}|\Psi_n\rangle \tag{9.31}$$

The integral of the ionic state with the neutral is

$$\chi_j(\vec{r}_N) := \int dr_1^{(3)}dr_{N-1}^{(3)}\left[\Phi^{(-j)}(r_1,\ldots,\vec{r}_{N-1})\right]\Psi(\vec{r}_1,\ldots,\vec{r}_{N-1},\vec{r}_N) \tag{9.32}$$

is the "Dyson orbital".

In terms of $|\chi_j\rangle$ we write

$$b^{-j}(\vec{k},t) = \int_0^t dt' \, e^{-i(\Delta E_j)(t-t')}e^{-i\Phi(\vec{k},t,t')}\langle\vec{k},t|\vec{r}|\chi_j\rangle. \tag{9.33}$$

This has exactly the same form as the single-electron SFA!

With these rather severe approximations, our multi-electron dipole response is the sum of independent responses form the relevant HOMO-j channels. If in zeroth approximation we assume that this is what happens, then each orbital can be considered an independent source of high harmonics, where only the few highest occupied orbitals contribute.

If we further use the factors ϕ instead of the Dyson orbitals χ_j, the cross-terms do not contribute, as the ϕ_j can be made orthogonal without loss of generality.

9.3.4 Interferences

So we have several sources of high harmonic radiation in the same spot, each giving the whole spectrum up to $\sim 3.17U_p + |E_j|$, and each radiating at its own particular phase! Clearly, the three sources will interfere. Note that all three sources can be considered point-like on the length scale of the harmonic radiation: the internuclear distance of CO_2 is a few $\rangle A$, while we are talking about harmonci wave length on the $\sim 30nm$ scale.

The phases determine whether the interference is constructive or destructive. If at least two sources are comparable in strenght, destructive interference an lead to a reduction of harmonic yield.

We need to compare phases for the same recombination energy

$$k_j^2/2 - E_j = k_{j'}^2/2 - E_{j'} \tag{9.34}$$

i.e. for *different* k_j. What determines the relative phases between the contributions

- The phase of re-combination: like the "atomic phase" in RABITT, the continuum-bound matrix element $\langle k_j|r|\chi_j\rangle$ has a k_j-dependent phase.
- The phase upon ionization. That is tricky: it is not obvious that an electron leaves from differnt χ_j with the same phase. Actually, we know from other sources, that differnt states may have different delays in XUV ionization, so why not in IR ionization? Nothing further is know about that.
- The Volkov phase accumulated: is also k_j-dependent!
- The difference of ionic energies $E_j - E_{j'}$, i.e. the relative beating of the ionic states while they are waiting for the electron to come back.

In addition, phase corrections to the plane wave must be taken into account. In the so-called eiconal approximation, these are the first corrections indicating deviation of the scattering solution from the plane wave. A more detailed desription of this correction can be found in O. Smirnova, M. Spanner and M. Yu. Ivanov, Phys. Rev. A, 77, 033407, (2008) (EVA- Eikonal Volkov Approximation).

With these basic ingredients, a model was built that can reprodruce the intensity-dependent shifts of the harmonic minima in CO_2.

Possible mixing of the ionic states by the field can also be described instead of using $U_i(t,t')$, let the field mix (but not distort) the ionic states. The effect of the mixing was reported to be negligible.

Bibliography

[1] P. Agostini, F. Fabre, G. Mainfray, G. Petite, and N. K. Rahman. Free-free transitions following six-photon ionization of xenon atoms. *Phys. Rev. Lett.*, 42:1127, 1997. 13

[2] M.V. Ammosov, N.B Delone, and V.P. Krainov. Tunnel ionization of complex atoms and of atomic ions in an alternating electromagnetic field. *Sov. Phys. JETP*, page 1191, 1986. 24

[3] E Constant, V D Taranukhin, A Stolow, and P B Corkum. Methods for the measurement of the duration of high-harmonic pulses. *Physical Review A*, 56:3870–3878, 1997. 80

[4] M Drescher, M Hentschel, R Kienberger, G Tempea, Ch. Spielmann, G Reider, P Corkum, and F Krausz. X-ray pulses approaching the attosecond frontier. *Science*, 291:1923, 2001. 70, 71

[5] M. Hentschel, R. Kienberger, C. Spielmann, G. A Reider, N. Milosevic, T. Brabec, P. Corkum, U. Heinzmann, M. Drescher, and F. Krausz. Attosecond metrology. *Nature*, 414:509, 2001. 70

[6] J Itatani, F Quere, G L Yudin, M Yu. Ivanov, F Krausz, and P B Corkum. Attosecond streak camera. *Physical Review Letters*, 88:173903, 2002. 80

[7] M Kitzler, N Milosevic, A Scrinzi, F Krausz, and T Brabec. Quantum Theory of Attosecond XUV Pulse Measurement .... *PRL*, 88:173904, 2002. 80

[8] Anne L'Huillier and Ph. Balcou. High-order harmonic generation in rare gases with a 1-ps 1053-nm laser. *Phys. Rev. Lett.*, 70(6):774–777, Feb 1993. 16

[9] Y. Mairesse and F. Quere. Frequency-resolved optical gating for complete reconstruction of attosecond bursts. *Phys. Rev. A*, 71:011401(R), 2005. 80

[10] H. G. Muller. Reconstruction of attosecond harmonic beating by interference of two-photon transitions. *Appl. Phys. B*, 74:S17, 2002. 80

[11] P M Paul, E S Toma, P Breger, G Mullot, F Auge, Ph. Balcou, H G Muller, and P Agostini. Observation of a train of attosecond pulses from high harmonic generation. *Science*, 292:1689–1692, 2001. 78, 80

[12] G. G. Paulus, F. Lindner, H. Walther, A. Baltuska, E. Goulielmakis, M. Lezius, and F. Krausz. Measurement of the phase of few-cycle laser pulses. *Phys. Rev. Lett.*, 91:253004, 2003. 26

[13] G. G. Paulus, W. Nicklich, Huale Xu, P. Lambropoulos, and H. Walther. Plateau in above threshold ionization spectra. *Phys. Rev. Lett.*, 72:2851–2854, May 1994. 14

[14] LM Perelomov, VS Popov, and MV Terentev. Ionization of atoms in an alternating electric field. *Sov. Phys. JETP*, 23:924–934, 1966. 24

[15] Rick Trebino. *Frequency-Resolved Optical Gating: The Measurement of Ultrashort Laser Pulses*. Springer Netherlands, 2002. 80

[16] Hugo W. van der Hart. Ionization rates for he, ne, and ar subjected to laser light with wavelengths between 248.6 and 390 nm. *Phys. Rev. A*, 73:023417, Feb 2006. 23

[17] Valérie Véniard, Richard Taïeb, and Alfred Maquet. Phase dependence of (n+1)-color (n>1) ir-uv photoionization of atoms with higher harmonics. *Phys. Rev. A*, 54:721–728, 1996. 75, 80